

CPon Dark Matter

Ferruccio Feruglio¹ * and Robert Ziegler^{1,2} §

¹INFN, Sezione di Padova, Via Marzolo 8, I-35131 Padua, Italy

²Institute for Theoretical Particle Physics, KIT, 76128 Karlsruhe, Germany

²Institute for Theoretical Physics, Heidelberg University, 69120 Heidelberg, Germany

Abstract

We study a class of supersymmetric models where the strong CP problem is solved through spontaneous CP violation, carried out by a complex scalar field that determines the Yukawa couplings of the theory. Assuming that one real component of this field - the CPon - is light, we examine the conditions under which it provides a viable Dark Matter candidate. The CPon couplings to fermions are largely determined by the field-dependent Yukawa interactions, and induce couplings to gauge bosons at 1-loop. All couplings are suppressed by an undetermined UV scale, which needs to exceed 10^{12} GeV in order to satisfy constraints on excessive stellar cooling and rare kaon decays. The CPon mass is limited from below by 5th force experiments and from above by X-ray telescopes looking for CPon decays to photons, leaving a range roughly between 10 meV and 1 MeV. Everywhere in the allowed parameter space the CPon can saturate the observed Dark Matter abundance through an appropriate balance of misalignment and freeze-in production from heavy SM fermions.

*E-mail: feruglio@pd.infn.it

§E-mail: robert.ziegler@kit.edu

1 Introduction

The nature of Dark Matter (DM) represents one of the most intriguing problems in contemporary physics [1]. Interpreted in terms of a new still undetected particle, DM can be explained by a variety of possible candidates, which have been the target of numerous experimental searches. For decades WIMPs have represented the reigning paradigm, supported by both the naturalness in reproducing the DM abundance and by the belief that low-energy supersymmetry could have offered the solution to the hierarchy problem. While the WIMP search is still very active today, the failure to detect supersymmetric partners at the LHC and the increasingly severe constraints on the WIMP-nucleon cross-section have gradually turned the attention to other DM candidates.

One of the most appealing possibilities is the QCD axion [2, 3], designed to solve the strong CP problem [4]. The axion is the pseudo-Goldstone boson of a global $U(1)_{\text{PQ}}$ anomalous symmetry. If infrared-dominated by QCD interactions, its dynamics relaxes the physical CP-violating $\bar{\theta}$ parameter to zero, whatever amount of CP violation might be stored in the quark mass matrices. In a wide range of parameter space, the axion is a viable candidate for cold DM, whose abundance is guaranteed, among other possibilities, by the misalignment mechanism [5–7]. A robust program of experimental axion searches is currently planned or underway [8]. A weak point of the axion solution to the strong CP problem is the quality problem, i.e. its excessive sensitivity to ultra-violet contributions to the energy density, particularly threatening in the context of a fundamental theory including gravity [9]. Also, the axion solution does not shed any light on the origin of fermion masses and mixing angles, unless the $U(1)_{\text{PQ}}$ symmetry is embedded in a larger flavor symmetry group explaining Yukawa hierarchies, see e.g. Refs. [10–14].

Recently, a new class of solutions to the strong CP problem has been proposed in Refs. [15, 16]. The ultraviolet theory is assumed to enjoy CP-invariance, spontaneously broken to deliver a nontrivial CKM phase while keeping $\bar{\theta}$ very small. Unlike the Nelson-Barr solution [17, 18], which also relies on the spontaneous breaking of CP, no additional heavy quark sector is required. Moreover, in their minimal implementation, these solutions assume a supersymmetric realization where the field content of the Minimal Supersymmetric Standard Model (MSSM) is minimally augmented to include a single extra gauge-invariant chiral supermultiplet τ ¹. A distinctive feature of the new solutions is that they provide a strict link between the origin of the fermion mass spectrum and the CP properties of both the weak and strong sectors of the theory.

All physical quantities depend on τ , whose vacuum expectation value (VEV) is the order parameter for the breaking of an anomaly-free flavour gauge symmetry that incorporates CP. The strong phase $\bar{\theta}$ vanishes in the supersymmetric limit, independently on the value of τ that determines the observed fermion masses, mixing angles and the weak CKM phase.

¹Another class of solutions of the strong CP problem relying on spontaneous CP violations makes use of discrete symmetries within a multiple Higgs doublet extension of the SM [19–21]. For further works on the solutions to the strong CP problem based on spontaneous CP violation, see e.g. [22–28].

If the mechanism of supersymmetry breaking does not introduce new physical phases or new flavour patterns, the observable $\bar{\theta}$ can remain very small. Supersymmetric particles have not been detected so far and an interesting possibility that we analyze in this work is that the only low-energy relic of this framework consists of a single spin-zero particle, here called CPon (pronounced as *cheap-on*), which can provide a viable DM candidate if sufficiently light.

The CPon shares several features with a CP-violating axion-like particle (ALP), with some important distinctions. Its interactions with all SM particles are non-renormalizable, suppressed by a large UV scale Λ taken as a free-parameter. For a sufficiently small mass $m_\xi < \text{MeV}$ and large Λ , the CPon can only decay into photons and/or neutrinos with a lifetime that easily exceeds the age of the Universe and can satisfy the stringent constraints on decaying DM from X-ray telescopes.

The CPon can be produced in the early universe by misalignment and thermal freeze-in [29] in a wide region of the parameter space (m_ξ, Λ) , similar to anomaly-free ALPs [30,31]. The allowed region is compact: the CPon mass m_ξ is bounded from below by precision tests of the gravitational inverse square law, and from above by limits on decaying DM. The UV scale Λ is limited from above by the Planck scale and bounded from below from limits on stellar cooling and SM decays with final state CPons (constraints on CPon-photon conversion in helio- and haloscopes are sub-leading). These limits depend on the CPon-fermion interactions, which are strictly related to the properties of the fermion mass spectrum, with some degree of model-dependence on the level of $\mathcal{O}(1 - 100)$ numbers.

In our analysis we keep the discussion as general as possible. Most of our results rely on few general properties and, when quantitative implications are derived, they make use of reasonable estimates based on dimensional analysis. Nevertheless, the most natural realization of the above scenario is within the framework of anomaly-free modular invariant flavour symmetries [15, 16, 32, 33]. Modular-invariant scalar potentials can deliver CP-violating minima [34–38]. Moreover, modular invariance, CP-invariance, and field dependence of observable quantities are all features expected in most 4-dimensional superstring compactifications, which can also allow for the possibility of a light scalar in the moduli mass spectrum, especially for ALP candidates [39–44]. In the final part of this work, we will analyze the prediction of a specific modular and CP invariant model, whose free parameters are fully determined by fitting fermion masses, mixing angle and the CKM phase.

In the context of modular invariant models, other DM candidates have been proposed, for instance a light axion [44, 45]. Another possible DM candidate is the lowest mass-state Dirac fermion, a combination of the Weyl components of driving ² and flavon supermultiplets [46]. Heavy moduli can play the role of DM portal, as discussed in Ref. [47]. In Nelson-Barr solutions to the strong CP problem, ultralight DM candidates have recently

²In models with flavor symmetries, driving fields are scalar fields introduced in the scalar potential to achieve the desired vacuum alignment.

been studied in Ref. [48]. Models unrelated to the strong CP problem, where a spin-zero component of the field responsible for spontaneous CP violation is a viable DM candidate have been discussed in Ref. [49].

This work is organized as follows. In Section 2 we discuss a broad class of models that solve the strong CP Problem by spontaneous CP violation, and introduce the CPon as the light real scalar within the CP-breaking field. Readers who are mainly interested in the CPon couplings to SM field can directly go to Eq. (2.12). In Section 3 we discuss various aspects of CPon phenomenology, in particular constraints from X-ray telescopes, rare flavor-violating SM decays, long range forces, star cooling and the neutron EDM. In Section 4 we discuss CPon production in the Early Universe by misalignment and freeze-in, and associated constraints from Warm DM. In Section 5 we specify two explicit benchmark scenarios, and discuss the resulting parameter space, before concluding in Section 6. In Appendix A we detail a model with modular-invariance as a complete framework for predicting CPon interactions.

2 A class of models solving strong CP

Our framework consists of a supersymmetric and CP-invariant theory, with the field content of the MSSM minimally extended to include a dimensionless gauge-invariant chiral supermultiplet τ [15, 16]³. The theory depends on the Kähler potential K , a real gauge-invariant function of the fields and their conjugates, the superpotential w and the gauge kinetic functions f_α ($\alpha = 1, 2, 3$), both gauge-invariant analytic functions of the chiral supermultiplets. All the physical quantities such as masses and coupling constants depend on the vacuum expectation value (VEV) of τ . Under CP, τ transforms as⁴

$$\tau \xrightarrow{CP} -\bar{\tau}, \quad (2.1)$$

so that real values of τ VEV are required to generate the CKM phase, via a spontaneous CP breaking. Before supersymmetry breaking, the physical angle $\bar{\theta}$, invariant under colored fermion chiral rotations, is

$$\bar{\theta} = -8\pi^2 \text{Im} f_3(\tau) + \arg \det Y_U(\tau) Y_D(\tau),$$

where $Y_{U,D}(\tau)$ are the matrices of Yukawa couplings in the up and down sectors⁵. It has been shown that, by requiring invariance of the theory under a suitable gauged flavour

³More such multiplets can be present, in general. Here we focus on the most economic realization where a single multiplet τ occurs.

⁴Up to possible discrete gauge symmetries of the theory acting on τ non-trivially. An equivalent formulation makes use of the field $T = -i\tau$, transforming as $T \rightarrow \bar{T}$ under CP.

⁵Notice that $\arg \det \mathcal{M}_U \mathcal{M}_D = \arg \det Y_U(\tau) Y_D(\tau)$, for any Kähler potential K , $\mathcal{M}_{U,D}$ denoting the quark mass matrices [50, 51].

symmetry, we can achieve the conditions [15, 16]:

$$\begin{aligned} f_\alpha(\tau) &= c_\alpha & (\alpha = 1, 2, 3) \\ \det Y_A(\tau) &= c_A & (A = U, D, E) \end{aligned} \quad (2.2)$$

where c_α and c_A are constants, required to be real by CP invariance. As a consequence, up to supersymmetry-breaking contributions, if $c_U c_D > 0$ we get $\bar{\theta} = 0$. Assuming a mechanism of supersymmetry breaking that does not generate either new phases or new flavour patterns, at low energy $\bar{\theta}$ is only corrected by tiny SM contributions [52, 53] and satisfies the experimental bounds. At the same time, a nontrivial dependence of $Y_{U,D}(\tau)$ on τ can deliver the observed CKM phase. No extra matter multiplets charged under the SM gauge group are needed and the real part of a single complex spin-zero field τ is sufficient to spontaneously break CP.

Within this general setup, we consider a scenario where the masses of the superpartners, including the fermionic component of the τ supermultiplet, are way bigger than the electroweak scale and their effects decouple at low energies. At the same time, we allow for the possibility that one of the two spin-zero components of the τ multiplet remains light and provides a Dark Matter (DM) candidate. In a general context, the scalar components of the τ multiplet are typically expected to be heavy, with masses potentially close to the scale Λ . However, if the framework under consideration represents (part of) the low-energy limit of a superstring compactification, τ could correspond to one of its moduli⁶. Moduli masses are suppressed by the gravitino mass $m_{3/2}$ and vanish in the limit of unbroken supersymmetry. Light moduli are therefore anticipated in scenarios where the gravitino mass is small [54], as in the case of gauge mediation, or in situations where the suppression is particularly pronounced. An example of the latter is the large volume scenario, where the mass of the volume modulus is proportional to $m_{3/2}(m_{3/2}/M_P)^{1/2}$ [55], M_P denoting the Planck mass. In both cases, moduli masses much smaller than one MeV can arise. The lightness of τ in this context is secured by supersymmetry, even though the relation between moduli masses and the supersymmetry breaking order parameter $m_{3/2}$ is model-dependent.

From $f_\alpha = c_\alpha$, we see that there are no tree-level couplings between τ and the SM gauge bosons. These can arise from loop corrections. All the relevant tree-level interactions are of Yukawa type. To identify such interactions, we start from the simple case of canonical Kähler potential. We expand the Yukawa term around the vacuum $\langle \tau \rangle$, keeping the first order in the fluctuation $\delta\tau/\Lambda$, Λ representing a convenient UV scale. Working in the limit of massless neutrinos, and neglecting a possible dependence of the Higgsino mass on τ , we get:

$$- \sum_A \psi_{Aa}^c m_{Aab} \psi_{Ab} - \frac{\delta\tau}{\Lambda} \sum_A \psi_{Aa}^c g_{Aab} \psi_{Ab} + \dots, \quad (2.3)$$

⁶Indeed, modular invariance is perhaps the more natural context to accommodate the relations in Eq. (2.2) [15].

where $v_E = v_D$. The sum extends over the three charge sectors ($A = U, D, E$) and, by denoting derivatives by an index, we have defined

$$m_{Aab} = \langle Y_{ab}^A(\tau) \rangle v_A \quad g_{Aab} = \langle Y_{\tau ab}^A(\tau) \rangle v_A. \quad (2.4)$$

The interactions of the complex field $\delta\tau$ are controlled by the scale Λ and by the matrices g_A , which, as a consequence of Eq. (2.2), satisfy the sum rule:

$$\text{tr}(m_A^{-1} g_A) = 0. \quad (2.5)$$

This sum rule is independent on the basis chosen for the fermion fields and plays an important role for phenomenology. In the following we further analyze its origin and show that it holds within a more general class of Kähler potentials.

2.1 A more general class of models

Without losing generality and in a matrix notation, the most general Kähler potential for quark and lepton supermultiplets φ_A and φ_A^c can be parametrized as

$$\sum_A \bar{\varphi}_A^c \Omega_A^{c\dagger} \Omega_A^c \varphi_A^c + \sum_A \bar{\varphi}_A \Omega_A^\dagger \Omega_A \varphi_A, \quad (2.6)$$

where Ω_A^c and Ω_A are matrices that depend on both τ and $\bar{\tau}$. By expanding the Kähler metric around the τ VEV, we can recover a canonical Kähler potential up to terms of second order in the fluctuations δ and $\bar{\delta}$ through the transformation

$$\varphi_A^c \rightarrow \langle \Omega_A^{c-1} \rangle (\mathbb{1} - \langle H_A^c \rangle \delta) \varphi_A^c \quad \varphi_A \rightarrow \langle \Omega_A^{-1} \rangle (\mathbb{1} - \langle H_A \rangle \delta) \varphi_A, \quad (2.7)$$

where

$$H_A^c = \Omega_{A\tau}^c \Omega_A^{c-1} + \Omega_A^{c\dagger-1} (\Omega_{A\bar{\tau}}^c)^\dagger, \quad H_A = \Omega_{A\tau} \Omega_A^{-1} + \Omega_A^{\dagger-1} (\Omega_{A\bar{\tau}})^\dagger. \quad (2.8)$$

In the new basis, the mass matrices m_A and couplings g_A of Eq. (2.3) read

$$m_A = \left\langle \Omega_A^{c-1T} Y^A \Omega_A^{-1} \right\rangle v_A, \quad g_A = \left\langle \Omega_A^{c-1T} Y_\tau^A \Omega_A^{-1} \right\rangle v_A - (\langle H_A^{cT} \rangle m_A + m_A \langle H_A \rangle), \quad (2.9)$$

When $\Omega_A^c = \Omega_A = \mathbb{1}$ the Kähler potential is canonical and we recover the previous case. In the general case, the first contribution to g_A is analogous to the one in Eq. (2.4) and automatically satisfies the sum rule of Eq. (2.5). The second contribution is due to the nontrivial dependence of the Kähler metric on τ . It also satisfies Eq. (2.5), provided

$$\det \Omega_A(\tau, \bar{\tau}) = \det \Omega_A^c(\tau, \bar{\tau}) = 1, \quad (2.10)$$

which represents the condition for the transformation (2.7) to be non-anomalous and to leave the gauge kinetic functions f_A unaffected. Important examples of this more general class are modular invariant theories, which will be further discussed in Section 5.2 and Appendix A. In anomaly-free modular invariant theories, the condition (2.10) can be naturally satisfied.

2.2 CPon interactions

The complex field $\delta\tau$ describes two real mass eigenstates, which are linear combinations of $\delta\tau$ and $\delta\bar{\tau}$. In the remaining part of this work, we assume that one of the two mass eigenstates is very heavy, with a mass of order Λ , while the other mass eigenstate, which we denote by ξ and refer to as CPon, has a mass $m_\xi \ll \Lambda$ that we treat as a free parameter. An angle α (with $0 \leq \alpha < \pi$) defines the direction ξ in the $(\delta\tau, \delta\bar{\tau})$ plane:

$$\xi = \frac{1}{\sqrt{2}}(e^{i\alpha}\delta\tau + e^{-i\alpha}\delta\bar{\tau}). \quad (2.11)$$

After moving to the basis where the fields are canonically normalized, in a four-component notation, the CPon interactions read:

$$\mathcal{L}_F = i\bar{\Psi}_A \gamma^\mu D_\mu \Psi_A - \bar{\Psi}_A \hat{m}_A \Psi_A - \frac{\xi}{\Lambda} \bar{\Psi}_A (y_S^A + i y_P^A \gamma_5) \Psi_A \left(1 + \frac{h}{\sqrt{2}v}\right) + \dots \quad (2.12)$$

for $A = U, D, E$ and the dots stand for terms of order ξ^2/Λ^2 . As we will see, Λ is bound to be very large, and terms of order ξ^2/Λ^2 can be safely neglected. We also show the CPon couplings to fermions and the Higgs boson h , which are relevant for CPon production in the early universe (in our conventions $v = 174 \text{ GeV}$). The fermion couplings are hermitian matrices in flavor space and given by

$$y_S^A = \frac{1}{2\sqrt{2}}(e^{-i\alpha}\hat{g}_A + e^{i\alpha}\hat{g}_A^\dagger), \quad y_P^A = \frac{i}{2\sqrt{2}}(e^{-i\alpha}\hat{g}_A - e^{i\alpha}\hat{g}_A^\dagger), \quad (2.13)$$

where the hat denotes matrices evaluated in the mass basis⁷. In general, both scalar and pseudoscalar interactions of ξ are present and the CPon behaves as a CP-violating ALP, with an important distinctive feature that we discuss in the next sections.

3 CPon Phenomenology

In this section we analyze the possible CPon decay channels and rates, a key aspect to account not only for CPon stability but also for the bounds on decaying DM coming from indirect X-ray and gamma-ray searches. We also discuss CPon production through

⁷The hat denotes the quantities evaluated in the mass basis, reached through the unitary transformation:

$$\Psi_A = \begin{pmatrix} \psi_A^c \\ \psi_A \end{pmatrix} \rightarrow \begin{pmatrix} U_{Ac} & 0 \\ 0 & U_A \end{pmatrix} \begin{pmatrix} \psi_A^c \\ \psi_A \end{pmatrix} \quad (A = U, D, E),$$

such that

$$U_{Ac}^T m_A U_A = \hat{m}_A \quad U_{Ac}^T g_A U_A = \hat{g}_A,$$

where \hat{m} is diagonal and positive definite.

scattering and decay processes initiated by SM particles, which is particularly relevant for determining the CPon abundance in the early universe and assessing constraints from rare flavour-violating decays with the CPon as missing energy. Finally, we analyze the limits on CPon couplings to ordinary matter (nucleons and electrons) from tests of the gravitational inverse square law and star cooling.

3.1 CPon decays

For CPon masses above threshold, the decay rate into an electron-positron pair scales approximately as $\Gamma_{\xi \rightarrow ee} \sim m_e^2 m_\xi / 8\pi \Lambda^2$. If this is the dominating decay channel, the CPon has a lifetime of about $10^{22} \text{ sec} \times (\Lambda/M_{\text{Pl}})^2 \times (10 \text{ MeV}/m_\xi)$. For Λ close to the Planck scale the CPon is cosmologically stable, but in conflict with CMB data that set a lower bound of about 10^{24} sec on the lifetime of a DM candidate decaying into e^+e^- , in a mass range from 1 MeV to 1 TeV [56]. We are thus led to restrict the CPon mass m_ξ to values smaller than about 1 MeV. In the limit of massless neutrinos, the only decay channel is into two photons⁸.

At the one-loop order, the amplitude for $\xi \rightarrow \gamma\gamma$ receives two contributions: one from a loop of electrically charged fermions and one from a loop of their scalar superpartners. If superpartners are very heavy, the latter can be neglected and we get (in agreement with e.g. Ref. [57–59]):

$$\Gamma_{\xi \rightarrow \gamma\gamma} = \frac{\alpha^2}{1024\pi^3} \frac{m_\xi^3}{\Lambda^2} (|c|^2 + |\tilde{c}|^2) , \quad (3.1)$$

where⁹:

$$\begin{aligned} c = & + \frac{8}{9} \left(4 \frac{y_{Suu}}{m_u} + \frac{y_{Sdd}}{m_d} + \frac{y_{Sss}}{m_s} \right) - \frac{1}{3} \left(\frac{y_{Suu} + y_{Sdd}}{m_u + m_d} + \frac{y_{Suu} + y_{Sss}}{m_u + m_s} \right) \\ & + \frac{28}{81} \left(\frac{y_{Suu}}{m_u} + \frac{y_{Sdd}}{m_d} + \frac{y_{Sss}}{m_s} \right) + \mathcal{O}(m_\xi^2/m_{e,\mu,\tau}^2) + \mathcal{O}(m_\xi^2/M_P^2) \end{aligned} \quad (3.2)$$

$$\tilde{c} = - \frac{1}{3} \frac{y_{Pee}}{m_e} \frac{m_\xi^2}{m_e^2} + \mathcal{O}(m_\xi^2/m_{\mu,\tau}^2) + \mathcal{O}(m_\xi^2/M_P^2) . \quad (3.3)$$

Compared to the leading part of the amplitude, the contribution of the scalar superpartners is suppressed by a relative factor of order $(m_t^2/m_{\text{SUSY}}^2)$, where m_{SUSY} denotes a representative superpartner mass. The coefficients c and \tilde{c} describe the CP-conserving and CP-violating part of the decay amplitude, respectively, and exhibit different behaviors. Both c and \tilde{c} are dimensionless and are expected to be proportional to y_{Saa}/m_a and y_{Paa}/m_a , at the leading order. Instead, in both c and \tilde{c} , the leptonic one-loop contribution

⁸In case of massive neutrinos, the CPon will decay mainly to neutrinos for CPon masses roughly below 1 keV. Still, its total lifetime is larger than 10^{24} sec for $m_\xi \leq 1 \text{ MeV}$ and $\Lambda = 10^{12} \text{ GeV}$ [30].

⁹In this section we omit the hat symbol to denote fermion masses.

is suppressed by the ratio m_ξ^2/m_ℓ^2 compared to the expected leading order behavior. This suppression is a direct consequence of the sum rule in Eq. (2.5), and resembles anomaly-free ALP models [30, 60–63]. A similar suppression takes place in the hadronic contribution to the CP-violating coefficient \tilde{c} , which is sourced by a small CPon- π^0 mixing. Thus, the coefficient \tilde{c} is dominated by the electron loop, whose result is explicitly shown in Eq. (3.2). Finally, the CP-conserving coefficient c receives two distinct hadron contributions: one from heavy quarks and one from light quarks and gluons. The former can be safely evaluated within the perturbative expansion, by computing the corresponding one-loop diagrams. The latter involves a non-perturbative regime associated with the light CPon mass. To estimate this part we re-elaborate the results of Refs. [64, 65] based on chiral perturbation theory¹⁰. By combining the heavy quark and light meson contributions, the leading-order term of the CP-conserving coefficient c does not exhibit any particular cancellation. The first three terms in Eq. (3.2) stand for: 1) the contribution from the heavy quarks t, c , and b expressed in terms of m_u, m_d and m_s using the sum rule in Eq. (2.5); 2) the contribution from π^\pm and K^\pm loops using chiral perturbation theory [65]; 3) the contribution from the ξ -gluon-gluon low-energy effective interaction (from integrating out heavy quarks) using low-energy theorems [64] and the sum rule in Eq. (2.5). As a result, the coefficient c is dominated by the quark sector, and the decay rate of the CPon into two photons is dominated by the CP-conserving part of the amplitude for CPon masses much below 1 MeV.

3.2 CPon production

Given the interactions of the CPon with SM fermions in Eq. (2.12), a light CPon can be produced from SM decays and scatterings, as well as from decays and scatterings of scalar superpartners. The latter processes are suppressed with respect to the former by at least m_f/m_{SUSY} , and most relevant for CPon production are flavor-violating decays $f_a \rightarrow f_b \xi$ and flavor-conserving $2 \rightarrow 2$ scattering processes $f_a \gamma \rightarrow f_a \xi$ and $f_a \bar{f}_a \rightarrow \gamma \xi$, and their QCD counterparts. While the scattering processes are only relevant for CPon production in the early universe, flavor-violating decays set very stringent bounds on CPon couplings, to be discussed in the next section. Here we collect the relevant expressions for the decay rates and cross-sections.

Production from SM decays From the general Lagrangian of Eq. (2.12) the decay rate for $f_a^A \rightarrow f_b^A \xi$ reads¹¹ in the limit $m_\xi = 0$

$$\Gamma_{f_a \rightarrow f_b \xi} = \frac{m_a}{16\pi} \left(1 - \frac{m_b^2}{m_a^2}\right) \left[\frac{|y_{Sba}|^2}{\Lambda^2} \left(1 + \frac{m_b}{m_a}\right)^2 + \frac{|y_{Pba}|^2}{\Lambda^2} \left(1 - \frac{m_b}{m_a}\right)^2 \right], \quad (3.4)$$

¹⁰We thank Gabriele Levati for his precious help in deriving the final result for the coefficients c and \tilde{c} .

¹¹We omit the A index, which is the same for initial and final states.

valid for charged lepton decays and flavour-violating transitions among heavy quarks. Taking also $m_b \ll m_a$, one obtains

$$\Gamma_{f_a \rightarrow f_b \xi} = \frac{m_a}{64\pi} \frac{|g_{ab}|^2 + |g_{ba}|^2}{\Lambda^2}, \quad (3.5)$$

with couplings g_{ab} defined in Eq. (2.9).

Production from SM $2 \rightarrow 2$ scattering processes In two-body scattering processes we only consider the dominant flavor-diagonal channels, with the following cross-sections:

$$\begin{aligned} \sigma_{f_a \gamma \rightarrow f_a \xi} = & \frac{\alpha_{\text{em}} Q_a^2}{8s(1-x)^3} \left[\frac{y_{Saa}^2}{\Lambda^2} (-x^4 + 6x^3 + 20x^2 - 22x - 2(3x+1)^2 \log x - 3) \right. \\ & \left. + \frac{y_{Paa}^2}{\Lambda^2} (1-x)^2 (-x^2 + 4x - 2 \log x - 3) \right], \end{aligned} \quad (3.6)$$

$$\begin{aligned} \sigma_{f_a \bar{f}_a \rightarrow \gamma \xi} = & \frac{\alpha_{\text{em}} Q_a^2}{s} \left[\frac{y_{Saa}^2}{\Lambda^2} \left(\frac{4x}{\sqrt{1-4x}} + (1-4x) \tanh^{-1}(\sqrt{1-4x}) \right) \right. \\ & \left. + \frac{y_{Paa}^2}{\Lambda^2} \frac{\tanh^{-1}(\sqrt{1-4x})}{1-4x} \right], \end{aligned} \quad (3.7)$$

where $x = m_a^2/s$ and Q_a denotes the electric charge of f_a . In the limit of $y_{Saa} = 0$ one recovers the expressions for derivatively coupled axions upon appropriate coupling identification, see e.g. Refs. [31, 66]. The corresponding scattering processes involving gluons and quarks, $\sigma_{q_a g \rightarrow q_a \xi}$ and $\sigma_{q_a \bar{q}_a \rightarrow g a}$, are obtained from these results by replacing $\alpha_{\text{em}} Q_a^2 \rightarrow \alpha_s/6$ in $\sigma_{f_a \gamma \rightarrow f_a a}$ and $\alpha_{\text{em}} Q_a^2 \rightarrow 4\alpha_s/9$ in $\sigma_{f_a \bar{f}_a \rightarrow \gamma a}$. Also relevant is scattering involving Higgs bosons, which in the limit of $\sqrt{s} \gg m_H, m_f$ has the cross-sections

$$\sigma_{f_a h \rightarrow f_a \xi}^0 = \sigma_{f_a \bar{f}_a \rightarrow h \xi}^0 = \frac{y_{Saa}^2 + y_{Paa}^2}{64\pi v^2 \Lambda^2} = \frac{|g_{aa}|^2}{128\pi v^2 \Lambda^2}, \quad (3.8)$$

which are not suppressed in the high-energy limit (as long as $\sqrt{s} \ll \Lambda$) in contrast to the ones involving gauge bosons above.

Also flavour-violating sfermion decays and scattering lead to CPon production, but their decay rates are suppressed compared to the corresponding processes involving fermions. The ratio of sfermion to fermions decay rates scales as m_f/m_{SUSY} , while the ratio of cross-sections scales as m_f^2/s , with $s > m_{\text{SUSY}}^2$. We thus neglect the SUSY contribution in the following.

3.3 Constraints from CPon decays

Electromagnetic decays of DM particles in the keV-MeV range are constrained by precision measurements of CMB temperature and polarization anisotropies, which give a bound on

the lifetime of roughly $\tau_{\gamma\gamma} \gtrsim 3 \times 10^{24}$ sec in the mass range of interest [56,67]. Even stronger constraints arise from searches for X-ray and low-energy gamma lines, which at present give limits on the partial width that are roughly three orders of magnitude more stringent than the CMB, depending on the precise mass range (with a weak dependence on the DM density profile [68,69]). Here we use the results collected in Appendix A of Ref. [30], which summarizes searches that have been conducted with Chandra [70,71], Newton-XMM [72], NuStar [73–76], and INTEGRAL [69]. These constraints are expected to further strengthen with future X-ray telescopes, and we use the optimistic projections collected in Ref. [30] for GECCO [77], THESEUS [78] and Athena [79–81], which could probe lifetimes of order 10^{30} sec for masses in the relevant mass range. For smaller masses there are limits from MUSE spectroscopic observations [82] (few eV), and the Hubble Space Telescope [83] (few tens of eV), which however for our benchmark models are weaker than limits from 5th experiments and RG stars, respectively. Instead relevant future limits are expected from exotic energy injection in the 21-cm power spectrum [84] for masses between few tens of eV and few keV.

These limits have to be compared to the prediction of the CPon decay rate into photons in Eq. (3.1), which is expected to be dominated by quark contribution. The total CPon decay rate into photons is then given by

$$\Gamma_{\xi \rightarrow \gamma\gamma} \approx \frac{1}{3.9 \times 10^{26} \text{sec}} \left(\frac{m_\xi}{\text{keV}} \right)^3 \left(\frac{10^{12} \text{GeV}}{\Lambda} \right)^2 |c|^2, \quad (3.9)$$

where

$$c \approx \frac{x_{uu}}{0.57 \text{MeV}} + \frac{x_{dd}}{4.7 \text{MeV}} + \frac{x_{ss}}{103 \text{MeV}}. \quad (3.10)$$

The value of c has been estimated using the light quark $\overline{\text{MS}}$ masses renormalized at 2 GeV: $m_u = 2.16$ MeV, $m_d = 4.70$ MeV and $m_s = 93.5$ MeV. This means that present constraints from CMB and X-ray searches exclude CPon masses above roughly 1 keV (for UV scales close to the present limits), with some prospects to probe lower masses with future X-ray telescopes and 21-cm cosmology.

3.4 Constraints from flavor-violating SM decays

As shown in Eq. (3.4), flavour-violating CPon couplings can induce rare decays with a CPon in the final state, which are severely constrained by current bounds on decays with missing energy (for a recent overview see Ref. [85]). The most important one is the decay $K^+ \rightarrow \pi^+ \xi$, which is constrained by the NA62 collaboration [86,87] at the level of $\text{BR}(K^+ \rightarrow \pi^+ X) \leq 5 \times 10^{-11}$ (90% CL), with X being a massless invisible particle. For the present scenario with a light CPon the predicted rate reads

$$\Gamma_{K^+ \rightarrow \pi^+ \xi} = \frac{|f_+^{K\pi}(0)|^2}{16\pi} \frac{|y_{Sds}|^2}{\Lambda^2} \frac{m_K^3}{(m_s - m_d)^2} \left(1 - \frac{m_\pi^2}{m_K^2} \right)^3, \quad (3.11)$$

where $f_+^{K\pi}(0) = 0.9698(17)$ [88–90], resulting in a branching ratio

$$\text{BR}(K^+ \rightarrow \pi^+ \xi) \approx 5 \times 10^{-11} \left(\frac{3.6 \times 10^{11} \text{ GeV}}{\Lambda} \frac{|y_{Sds}|}{\sqrt{m_d m_s}} \right)^2. \quad (3.12)$$

Here we have normalized y_{Sds} to the natural value expected in simple scenarios, see Section 5. Since this value can also be easily enhanced by a numerical factor as large as $\mathcal{O}(100)$, we find that typically one needs $\Lambda \gtrsim 10^{11} \div 10^{13}$ GeV in order to be consistent with NA62 searches. This result is essentially independent of the CPon mass, as long as it is below the experimental resolution of about few MeV. With the full data set NA62 will be sensitive to 2-body branching ratios of about 10^{-11} [91], which gives a projected limit on the UV scale that is large by roughly factor two.

Another important channel is the decay $\mu^+ \rightarrow e^+ X$, which has a signature similar to the SM decay, but with 2-body kinematics. To distinguish signal from background one can employ polarized decays, which are sensitive to the ratio of scalar to pseudo-scalar couplings [92]. Unless these couplings are aligned to the SM (i.e. have a V-A structure), the most stringent constraint comes from the Iodidio experiment at TRIUMF [93], giving a 90% CL bound $\text{BR}(\mu^+ \rightarrow e^+ X) \leq 2.5 \times 10^{-6}$ for a massless X boson. For complete alignment the bound would be loosened to $\text{BR}(\mu^+ \rightarrow e^+ X) \leq 5.8 \times 10^{-5}$, according to searches by the TWIST collaboration [94]. Interestingly, these bounds may be further strengthened in the near future at MEG-II [92, 95], Mu3e [96] and Mu2e or COMET [97], probing 2-body branching ratios up to 7×10^{-8} [92]. In our setup, we get from Eq. (3.5)

$$\text{BR}(\mu^+ \rightarrow e^+ X) \approx \frac{3\pi^2}{G_F^2 m_\mu^4} \frac{|g_{e\mu}|^2 + |g_{\mu e}|^2}{\Lambda^2} \approx 2.5 \times 10^{-6} \left(\frac{2.6 \times 10^8}{\Lambda} \frac{g_{e\mu, \mu e}}{\sqrt{2m_e m_\mu}} \right)^2, \quad (3.13)$$

where we have neglected the electron mass and restricted for simplicity to couplings not aligned to the SM. We also introduced the shorthand notation $g_{e\mu, \mu e} \equiv \sqrt{|g_{e\mu}|^2 + |g_{\mu e}|^2}$, which we have again normalized to the natural value expected in simple scenarios. Even taking into account large numerical enhancement factors, it is clear that the stringent constraints on $K^+ \rightarrow \pi^+ \xi$ prevent large effects in $\mu^+ \rightarrow e^+ \xi$ (even at future experimental facilities), unless there is a pronounced hierarchy between the couplings in the quark and charged lepton sectors. Similar considerations for other sectors, e.g. flavor-violating τ - or B-meson decays constrained by Belle II [91, 98, 99], show that such processes are also strongly limited by the large value of Λ needed to suppress $b \rightarrow d$ transitions. Moreover, as we discuss in the next sections, astrophysical constraints yield limits on Λ on the same level as NA62, but are somewhat less model-dependent since they involve only flavor-diagonal couplings. Therefore only $K \rightarrow \pi$ decays are relevant, especially if the corresponding couplings involve large numerical enhancement factors.

3.5 Constraints from long range forces

If the CPon is very light and has sufficiently large couplings to ordinary matter, it can mediate long-range forces that violate the inverse-square law (ISL), or the equivalence principle (EP), or both. The relevant interactions are the scalar ones, described by the y_S^A terms in Eq. (2.12), inducing spin-independent effects. For pseudoscalars interaction, described by the y_P^A parameters, spin-dependent effects would arise from the exchange of ξ in the non-relativistic limit. Even if the mass of the CPon is very small or exactly zero, it does not mediate a long-range force between unpolarized bodies¹².

In a system of two static test bodies with masses $m_{1,2}$ at a distance r , the deviation from the Newton potential (ISL) are usually parametrized by:

$$\delta V_{ISL}(r) = -\frac{Gm_1m_2}{r}\alpha e^{-r/\lambda}. \quad (3.14)$$

The exchange of a light CPon gives rise to a modification to the Newton potential:

$$\delta V(r) = -\frac{y_{SNN}^2}{4\pi\Lambda^2 r} N_1 N_2 A_1 A_2 e^{-m_\xi r} + \dots, \quad (3.15)$$

for two test bodies containing $N_{1,2}$ atoms of mass numbers $A_{1,2}$ experiencing a scalar CPon-nucleon interaction

$$\mathcal{L} \supset -\frac{\xi}{\Lambda} y_{SNN} \bar{N} N, \quad (3.16)$$

and the dots above stand for additional smaller contributions arising from CPon-electron interactions. By making use of the identification

$$\lambda = \frac{1}{m_\xi}, \quad \alpha = \frac{y_{SNN}^2}{4\pi G \Lambda^2 u^2}, \quad (3.17)$$

with $u = 0.9315$ GeV being the atomic mass unit, we can obtain corresponding upper bounds on the coupling constant y_{SNN} using the experimental limits on λ and α . For our purposes most relevant are the constraints in the mass range $\text{meV} < m_\xi < 10 \text{ eV}$ (or length scales $100 \mu\text{m} < \lambda < 10 \text{ nm}$), which have been obtained by test of the ISL, while EP tests are sensitive only to much smaller CPon masses. Here we use the combined limits from Ref. [100], obtained from results using a torsional oscillator at the Indiana University-Purdue University Indianapolis (“IUPUI”) [101], torsion balance tests (“Eöt-Wash”) [102, 103] and torsion pendula at the Huazhong University of Science and Technology (“HUST”) [104–107].

To convert these limits into constraints in the plane (m_ξ, Λ) , we need the relation between the scalar CPon-nucleon couplings y_{SNN} and the scalar CPon-quark couplings $y_{S,aa}^{U,D}/\Lambda$ in Eq. (2.12). The leading contribution to the CPon-nucleon coupling, arising

¹²Limits from experiments with polarized bodies can be found in Ref. [100]. They are less constraining than those discussed here.

from heavy quarks via the triangle diagram with external gluons, has been evaluated in Ref. [108], giving:

$$y_{SNN} = \frac{2m_N}{27} \sum_{q=c,b,t} \frac{y_{Sq\bar{q}}}{m_q}. \quad (3.18)$$

A more refined estimate, including also the contribution of the light quarks, is derived in Ref. [109]. It modifies the value of y_{SNN} by approximately 30% for the benchmark values of $y_{Sq\bar{q}}$ in Section 5. For an order-of-magnitude evaluation, we use the relation of Eq. (3.18), as anyway the limits we obtain on Λ depend on the model-dependent value of $y_{Sq\bar{q}}$. Within this approximation, protons and neutrons have the same couplings to the CPon. Taking the natural value for $y_{Sq\bar{q}} \sim m_q$, we find $y_{SNN} \sim 0.2 \text{ GeV}$, so that the bounds from ISL tests restrict Λ to be above $(10^{19} \div 10^{13}) \text{ GeV}$ in the mass range $(10^{-3} \div 1) \text{ eV}$ [100]. As discussed in Section 5, these limits can easily strenghtened up to two orders of magnitude, to the presence of large numerical enhancement factors. Requiring Λ to be below the Planck scale thus means that the CPon has to be heavier than about 10^{-9} MeV .

In the above discussion we have neglected the contribution to $\delta V(r)$ arising from CPon exchange between electrons, which is obtained by replacing $y_{SNN}^2 N_1 N_2 A_1 A_2$ with $y_{See}^2 N_1 N_2 Z_1 Z_2$, in Eq. (3.15), with $Z_{1,2}$ denoting the atomic numbers of the two test bodies. Such a contribution is therefore parametrically suppressed with respect to the one in Eq. (3.15) by a factor $(y_{See}/y_{Stt})^2 (m_t/m_N)^2 \approx m_e^2/m_N^2$.

3.6 Constraints from star cooling

For masses much below 1 MeV the CPon is light enough to be thermally produced in stellar plasmas. Unless the couplings to ordinary matter (electrons and nucleons) are sufficiently small, this leads to an excessive energy loss in the form of long-lived CPons, which is strongly constrained by observations of various stellar systems [110]. Here we use the constraints obtained in Ref. [111, 112] to set limits on scalar couplings to electron and nucleons, due to CPon production in White Dwarfs (WDs), affecting observations of the WD luminosity function. These limits are effective up to CPon masses of about 1 keV, where production becomes Boltzmann-suppressed, and restrict the scalar couplings to electrons to $y_{See}/\Lambda \lesssim 4 \times 10^{-16}$ and nucleons to $y_{SNN}/\Lambda \lesssim 7 \times 10^{-13}$. For natural values of the couplings, $y_{See} \sim m_e$ and $y_{SNN} \sim 0.2 \text{ GeV}$, it is clear that the WD limits require $\Lambda \gtrsim 10^{12} \text{ GeV}$ for CPon masses below $\sim 1 \text{ keV}$. Constraints from Red Giants (RGs), first studied in Ref. [113], extend to slightly higher temperatures¹³ of about $\sim 10 \text{ keV}$, and we use the limits¹⁴ provided in Ref. [114], which constrain scalar couplings to electrons at the

¹³Limits from Horizontal Branch stars extend to even larger masses, but are too weak to be relevant in our scenario.

¹⁴These results have been criticized by the authors of Ref. [111], arguing that they are based on the assumption of non-degenerate and non-relativistic electrons, which is not a good approximation. Nevertheless this should affect the limits on the couplings only at the level of $\mathcal{O}(1)$ factors.

level of $y_{See}/\Lambda \lesssim 7 \times 10^{-16}$ and couplings to nucleons at the level $y_{SNN}/\Lambda \lesssim 1 \times 10^{-12}$. Note that these limits are much stronger than those from e.g. helioscopes [115].

3.7 Constraints from the neutron EDM

As a result of the conditions in Eq. (2.2), $\bar{\theta}$ (and thus the neutron EDM) vanishes as long as supersymmetry remains unbroken. Small enough corrections to $\bar{\theta}$ from supersymmetry breaking can be guaranteed under appropriate conditions. Denoting by Λ_{SUSY} the scale at which supersymmetry breaking is mediated to the observable sector, and by m_{SUSY} the sparticle mass scale, a favorable framework is achieved when $\Lambda \gg \Lambda_{\text{SUSY}} \gg m_{\text{SUSY}}$ [50, 51]. At the UV scale Λ the observable $\bar{\theta}$ vanishes and it receives no quantum corrections down to Λ_{SUSY} as a consequence of supersymmetric nonrenormalization theorems [116]. Assuming that the whole supermultiplet τ is heavier than Λ_{SUSY} , it can be integrated out without modifying the quark masses. Corrections below Λ_{SUSY} , due to RG running of soft terms and from integrating out sparticles at the scale m_{SUSY} are model-dependent and can be kept below the observable level by assuming that supersymmetry breaking is gauge-mediated [117] or anomaly-mediated [118–120]. Finally, corrections due to the CKM phase [52, 53] are known to be negligibly small.

In our scenario, these conditions are altered by the fact that one real component of the τ supermultiplet remains light and the remaining ones have a mass of order m_{SUSY} . Corrections to $\bar{\theta}$ are then expected by both integrating out the heavy components of τ , namely a real spin-zero particle and a Majorana fermion, and by loop corrections involving a CPon exchange. All these corrections affect $\bar{\theta}$ through a shift of the quark mass matrix, $m_q \rightarrow m_q + \delta m_q$, which results in the shift

$$\delta \bar{\theta} = \text{Im tr}(m_q^{-1} \delta m_q). \quad (3.19)$$

The most important shift δm_q arises at one-loop and is necessarily quadratic in $1/\Lambda$, since it involves the emission and absorption of a τ component with couplings $\propto 1/\Lambda$. On dimensional grounds, we expect contributions of the type

$$\delta \bar{\theta} \approx \frac{L}{16\pi^2} \left\{ \frac{v^2}{\Lambda^2}, \frac{v m_{\text{SUSY}}}{\Lambda^2}, \frac{m_{\text{SUSY}}^2}{\Lambda^2} \right\}, \quad (3.20)$$

where L denotes a combination of dimensionless coupling constants, mass ratios, and logarithms¹⁵. The largest set of corrections comes from the third term in Eq. (3.20). Upper bounds on the neutron EDM require $\delta \bar{\theta} \leq 10^{-10}$ [122, 123], which translate into an upper limit on the sparticle mass scale

$$m_{\text{SUSY}} < \frac{1.3 \times 10^8}{\sqrt{L}} \left(\frac{\Lambda}{10^{12} \text{ GeV}} \right) \text{ GeV}. \quad (3.21)$$

¹⁵See, for example, Ref. [121].

At the border of the region allowed by stellar cooling, namely $\Lambda \approx 10^{12}$ GeV, even considering values of L up to 10^6 , m_{SUSY} can be as large as 10^5 GeV, without spoiling the solution to the strong CP problem. This makes also clear that the $\delta\bar{\theta}$ contributions $\propto v^2/\Lambda^2$ are entirely harmless, due to the strong suppression of the UV scale Λ .

4 Dark matter abundance

As discussed in Section 3.1, the CPon has a lifetime that easily exceeds the age of the universe, and thus is a viable DM candidate. Since its couplings to SM particles are extremely suppressed ($\Lambda \gtrsim 10^{12}$ GeV from star cooling constraints), the CPon is not in thermal contact with the SM thermal in the early universe, and thus CPon freeze-out production via thermal freeze-out is not an option. Instead a CPon abundance can be produced in the early universe via a variety of mechanisms, here we restrict for simplicity to thermal freeze-in, which is suggested by the smallness of CPon couplings to the SM, and vacuum misalignment.

4.1 Vacuum misalignment

Scalar DM fields are generically produced in the early universe through the misalignment mechanism [124–126], which generalizes the classic scenario for production of the QCD axion [5–7]. The equation of motion of a scalar field in an expanding universe is given by

$$\ddot{\xi} + 3H(T)\dot{\xi} + m_\xi^2\xi = 0, \quad (4.1)$$

where we restricted to a quadratic CPon potential, and H is the Hubble parameter. At early times, the CPon field is frozen at some initial value ξ_0 that we parametrize in terms of the UV scale Λ as $\xi_0 = \Lambda\theta_0$ (note that the real parameter θ_0 is not a periodic variable). We expect ξ_0 to remain below the cutoff scale of our effective theory, which is of the order of Λ . Consequently, θ_0 cannot significantly exceed a value of one. We assume that the CPon is present before inflation, so that the value θ_0 is uniform across the Hubble patch that forms up the observable universe today. As the universe cools, the CPon starts oscillating, which happens around $m_\xi \sim H(T_{\text{osc}})$. We take the condition $m_\xi = 1.6H(T_{\text{osc}})$ to determine T_{osc} , which provides a good fit to the results of a numerical integration [125]. The energy stored in these oscillations behaves just as cold DM, so that today's abundance can be obtained from rescaling the energy density at the onset of oscillations $\rho_\xi = 1/2m_\xi^2\Lambda^2\theta_0^2$ by the ratio of entropy densities today and the onset of oscillations $s_0/s(T_{\text{osc}})$.

The final CPon abundance depends on the cosmological scenario at the time of oscillations. For sufficiently high reheating temperatures oscillations start during the epoch of radiation domination (RD). With $H_{\text{RD}} = T^2/M_{\text{Pl}}1.66\sqrt{g_*}$ one obtains

$$T_{\text{osc}}^{\text{RD}} = 6.7 \times 10^5 \text{ GeV} \left(\frac{m_\xi}{\text{keV}} \right)^{1/2}, \quad (4.2)$$

where we took $g_*(T_{\text{osc}}) = 106.75$. The final CPon abundance in RD is then

$$\Omega_\xi h^2|_{\text{mis}}^{\text{RD}} \approx 0.12 \left(\frac{\Lambda\theta_0}{1.1 \times 10^{11} \text{ GeV}} \right)^2 \left(\frac{m_\xi}{\text{keV}} \right)^{1/2}, \quad (4.3)$$

and this expressions are valid for $T_R \geq T_{\text{osc}}^{\text{RD}}$. If instead the reheating temperature is smaller than $T_{\text{osc}}^{\text{RD}}$, we assume a period of early matter domination (EMD), where $H_{\text{EMD}} = H_{\text{RD}} \times T^2/T_R^2 \sqrt{g_*/g_*(T_R)}$ [127]. In this case CPon oscillations start at

$$T_{\text{osc}}^{\text{EMD}} = 1.2 \times 10^5 \text{ GeV} \left(\frac{m_\xi}{\text{keV}} \right)^{1/4} \left(\frac{T_R}{18 \text{ TeV}} \right)^{1/2}, \quad (4.4)$$

and the relic abundance is independent of the CPon mass and given by

$$\Omega_\xi h^2|_{\text{mis}}^{\text{EMD}} \approx 0.12 \left(\frac{\Lambda\theta_0}{6.7 \times 10^{11} \text{ GeV}} \right)^2 \left(\frac{T_R}{18 \text{ TeV}} \right). \quad (4.5)$$

In the following we will treat the reheating temperature as a free parameter above 10 MeV, which slightly exceeds the lower limit allowed by Big-Bang-Nucleosynthesis (BBN) [128, 129].

4.2 Freeze-in

Even for very weak interactions, unable to keep the CPon in equilibrium with the plasma in the early universe, DM particles will be produced by cumulative decays and scatterings of SM particles in the thermal bath. This mechanism for building up a DM abundance of the observed size goes under the name of ‘‘Thermal Freeze-in’’ [29]. Below we briefly review the basis formalism that allows to relate the DM relic abundance to the model parameters, following the original reference [29], see also the appendices in Refs. [130, 131].

Boltzmann equation The number density n_ξ of CPons is determined by the integrated Boltzmann equation (see e.g. Ref. [132])

$$\frac{dn_\xi}{dt} + 3Hn_\xi = \left(n_\xi^{\text{eq}} - n_\xi \right) \sum_i \Gamma_i, \quad (4.6)$$

where $n_\xi^{\text{eq}} = 0.122 T^3$ is the CPon equilibrium number density, H is the Hubble parameter $H = T^2/M_{\text{Pl}} 1.66 \sqrt{g_*(T)}$ with $g_*(T)$ denoting the total number of relativistic degrees of freedom and Γ_i are the specific CPon production rates, which are related to the respective collision terms \mathcal{C}_i by $\Gamma_i = \mathcal{C}_i/n_\xi^{\text{eq}}$.

Entropy conservation ($d(sa^3)/dt = 0$) allows to rewrite the time derivative in terms of a derivative with respect to temperature as $dT/dt = -HT$, which is valid when the effective

number of relativistic entropy degrees of freedom is approximately constant, $dg_{*s}(T)/dT \approx 0$. This relation can be used to rewrite the Boltzmann equation in terms of the CPon yield $Y_\xi = n_\xi/s$, giving

$$\frac{dY_\xi}{dT} = - \left(1 - \frac{Y_\xi}{Y_\xi^{\text{eq}}} \right) \sum_i \frac{\mathcal{C}_i(T)}{sTH}, \quad (4.7)$$

with the entropy density $s = 0.439 T^3 g_{*s}(T)$. In the freeze-in regime the CPons are never in thermal equilibrium, $Y_\xi \ll Y_\xi^{\text{eq}}$, and their initial abundance at T_R can be neglected. Thus the final yield Y_ξ^0 of CPons today (at $T \approx 0$) is given by the integral

$$Y_\xi^0 = \sum_i \int_0^{T_R} \frac{\mathcal{C}_i(T)}{sTH} dT = \sum_i \frac{1.4}{g_{*s}\sqrt{g_*}} \int_0^{T_R} \frac{\mathcal{C}_i(T) M_{\text{Pl}}}{T^6} dT, \quad (4.8)$$

where the effective number of relativistic degrees of freedom are evaluated at the characteristic temperature of the production process, which for decays is the mass of the decaying particle and for scattering processes the threshold center-of-mass energy (unless the process is UV sensitive, in which case it is $T_{\text{max}} = T_R$ [29, 133]). The final CPon abundance is thus given by multiplying the yield by $m_\xi s_0/\rho_{\text{crit}}$, giving

$$\Omega_\xi h^2 = m_\xi \sum_i \frac{4.6 \times 10^{27}}{g_{*s}\sqrt{g_*}} \int_0^{T_R} \frac{\mathcal{C}_i(T)}{T^6} dT. \quad (4.9)$$

Collision terms The form of the collision terms depend on the underlying production process. The relevant process here are flavor-violating decays $f_a \rightarrow f_b \xi$, flavor-diagonal scatterings with photons (or gluons), $f_a \gamma \rightarrow f_a \xi$, fermion annihilations to CPons and photons (or gluons) $f_a \bar{f}_a \rightarrow \xi \gamma$, and finally scattering on Higgs bosons, $f_a h \rightarrow f_a \xi$ and $f_a \bar{f}_a \rightarrow \xi h$ (in the high-energy limit). The respective collision terms read in terms of the expressions in Section 3.2 (using Maxwell-Boltzmann instead of Fermi-Dirac distributions):

$$\mathcal{C}_{f_a \rightarrow f_b \xi} = \frac{T m_a^2}{\pi^2} K_1 \left(\frac{m_a}{T} \right) \Gamma_{f_a \rightarrow f_b \xi}, \quad (4.10)$$

$$\mathcal{C}_{f_a \gamma \rightarrow f_a \xi} = \frac{T}{8\pi^4} \int_{m_a^2}^{\infty} \left(1 - \frac{m_a^2}{s} \right)^2 s^{3/2} \sigma_{f_a \gamma \rightarrow f_a \xi}(s) K_1 \left(\frac{\sqrt{s}}{T} \right) ds, \quad (4.11)$$

$$\mathcal{C}_{f_a \bar{f}_a \rightarrow \gamma \xi} = \frac{T}{8\pi^4} \int_{4m_a^2}^{\infty} \left(1 - \frac{4m_a^2}{s} \right) s^{3/2} \sigma_{f_a \bar{f}_a \rightarrow \gamma \xi}(s) K_1 \left(\frac{\sqrt{s}}{T} \right) ds, \quad (4.12)$$

$$\mathcal{C}_{f_a \bar{f}_a \rightarrow h \xi} = 2\mathcal{C}_{f_a h \rightarrow f_a \xi} = \frac{T}{8\pi^4} \int_0^{\infty} s^{3/2} \sigma_{f_a \bar{f}_a \rightarrow h \xi}^0 K_1 \left(\frac{\sqrt{s}}{T} \right) ds, \quad (4.13)$$

where the factor of 2 in the last line is due to the different spin degrees of freedom, and $K_1(x)$ denotes the modified Bessel function of the second kind. Expressions for gluons instead of photons are analogous.

Relic abundancies The temperature integral for the decays can readily be performed, and are dominated by the region where $T \approx m_a$, giving $\int K_1(m_a/T)/T^5 dT \propto m_a^{-4}$ for dimensional reasons (as long as $T_R \gg m_a$). Similarly one can do the temperature integral for the scatterings involving vector bosons, as the remaining s -integral is convergent in the UV due to $\sigma_i \propto 1/s$ and can be done analytically. Instead the scattering on Higgs bosons is UV sensitive as the cross-section is constant, so one has first to perform the s -integral, giving $\int s^{3/2} K_1(\sqrt{s}/T) \propto T^5$, and then perform the temperature integral which is linearly divergent and thus given by T_{\max} (this justifies to work in the limit $\sqrt{s} \gg m_H, m_a$). The result for the integrated collision terms read

$$\int_0^\infty \frac{\mathcal{C}_{f_a \rightarrow f_b \xi}(T)}{T^6} dT = \frac{3}{2\pi} \frac{\Gamma_{f_a \rightarrow f_b \xi}}{m_a^2} = \frac{3}{128\pi^2 m_a \Lambda^2} (|g_{ab}|^2 + |g_{ba}|^2), \quad (4.14)$$

$$\int_0^\infty \frac{\mathcal{C}_{f_a \gamma \rightarrow f_a \xi}(T)}{T^6} dT = \frac{\alpha_{\text{em}} Q_a^2}{168\pi^3 m_a \Lambda^2} ((63\pi^2 - 600)y_{Saa}^2 + 16y_{Paa}^2), \quad (4.15)$$

$$\int_0^\infty \frac{\mathcal{C}_{f_a \bar{f}_a \rightarrow \gamma \xi}(T)}{T^6} dT = \frac{\alpha_{\text{em}} Q_a^2}{160\pi^2 m_a \Lambda^2} (13y_{Saa}^2 + 15y_{Paa}^2),$$

$$\int_0^{T_R} \frac{\mathcal{C}_{f_a \bar{f}_a \rightarrow h \xi}(T)}{T^6} dT = \frac{4T_R}{\pi^4} \sigma_{f_a \bar{f}_a \rightarrow h \xi}^0 = \frac{T_R}{32\pi^5 v^2 \Lambda^2} |g_{aa}|^2. \quad (4.16)$$

As the couplings scale as $y_{Paa} \sim y_{Saa} \sim g_{aa} \sim g_{ab} \sim g_{ba} \sim m_a$, the dominant contribution comes from the top quark (provided $T_R > m_t$), and the scattering on gluons instead of photons, which are analogous with $\alpha_{\text{em}} Q^2 \rightarrow 24 \times \alpha_s(m_t)/6$ in $tg \rightarrow t\xi$ and $\alpha_{\text{em}} Q^2 \rightarrow 9 \times 4\alpha_s(m_t)/9$ in $t\bar{t} \rightarrow g\xi$, where the first factors compensate for the color averaging in the definition of the cross-section. The effective number of relativistic degrees of freedom in Eq. (4.9) is then given by $g_* = 106.75$ for all processes. Note that CPon production from SUSY scattering on gauge bosons is suppressed by at least m_t/m_{SUSY} , but SUSY scattering on Higgs bosons is not, provided that $T_R > m_{\text{SUSY}}$, i.e. supersymmetric partners are in thermal equilibrium with the SM bath. Here we neglect this contribution, which depends on details of the supersymmetric spectrum, having in mind a scenario where this condition is not satisfied.

Normalizing to the natural values of the couplings (see Section 5), we finally obtain for the CPon relic abundancies, taking into account a possible factor of two for the charge-conjugated process,

$$\Omega_\xi h^2|_{t-\text{decays}} = 0.12 \left(\frac{m_\xi}{\text{keV}} \right) \left(\frac{9.2 \times 10^9 \text{ GeV}}{\Lambda} \right)^2 \left(\frac{\sqrt{|g_{ct}|^2 + |g_{tc}|^2}}{300 \text{ GeV}} \right)^2 \left(\frac{172 \text{ GeV}}{m_t} \right),$$

$$\Omega_\xi h^2|_{t-\text{scat(IR)}} = 0.12 \left(\frac{m_\xi}{\text{keV}} \right) \left(\frac{1.4 \times 10^{11} \text{ GeV}}{\Lambda} \right)^2 \left(\frac{|g_{tt}|}{5.2 \text{ TeV}} \right)^2 \left(\frac{172 \text{ GeV}}{m_t} \right) \left(\frac{\alpha_s(m_t)}{0.11} \right),$$

$$\Omega_\xi h^2|_{t-\text{scat(UV)}} = 0.12 \left(\frac{m_\xi}{\text{keV}} \right) \left(\frac{1.4 \times 10^{11} \text{ GeV}}{\Lambda} \right)^2 \left(\frac{|g_{tt}|}{5.2 \text{ TeV}} \right)^2 \left(\frac{T_R}{3.1 \text{ TeV}} \right), \quad (4.17)$$

where we restricted to $t \rightarrow c$ decays and took for simplicity $y_{Ptt} \approx y_{Stt} \approx |g_{tt}|/2$. From these results it is clear that decays are typically subleading to IR scattering, and UV scattering dominates over IR scattering if $T_R \gtrsim 3.1$ TeV. These expressions are valid as long as $m_t \ll T_R < \Lambda$, while for reheating temperatures below the EW scale the main contribution to the freeze-in abundance occurs either from top scattering during the EMD epoch, which leads to a strong dilution of the resulting abundance (see e.g. Ref. [134]), or from scattering of lighter fermions, for which the abundance is suppressed by small couplings. For simplicity we simply set the freeze-in contribution to zero for $T_R < 200$ GeV, since it anyway has no impact in the relevant region of parameter space, see Section 5.3. Moreover we need to restrict to $T_R < \Lambda$, as the EFT we have used to calculate CPon production rates is valid only for energies below the UV cutoff Λ .

4.3 Limits on Warm Dark Matter

While misalignment produces CPon DM with essentially vanishing momentum, CPons created by freeze-in have a large initial velocity and are initially free-streaming. This leads to a suppression of primordial fluctuations imprinted in the matter power spectrum at small scales, which can be constrained by looking at the spectra of distant quasars distorted by absorption in neutral hydrogen filaments that are assumed to trace the matter power spectrum, usually referred to as the Lyman- α forest (Ly- α) [135, 136]. This analysis yields a stringent lower bound on the warm DM mass $m_{\text{WDM}}^{\text{min}} \approx 5.3$ keV [137–139], which can be relaxed to $m_{\text{WDM}}^{\text{min}} \approx 3.5$ keV under more conservative assumptions. These Ly- α limits have been recasted for different freeze-in processes by computing the exact DM velocity distribution in Refs. [140–142]. As we will show below, most relevant for our scenario is production via UV freeze-in which results in the “Warm Dark Matter” (WDM) constraint [141]

$$m_\xi \gtrsim 7 \text{ keV} \left(\frac{m_{\text{WDM}}^{\text{min}}}{3 \text{ keV}} \right)^{4/3} \left(\frac{106.75}{g_*(T_R)} \right)^{1/3}, \quad (4.18)$$

where $m_{\text{WDM}} \approx 3.5$ keV or 5.3 keV for the conservative and stringent bounds, respectively, and T_R denotes the reheating temperature. This bound gets relaxed if freeze-in gives only a small fraction of a total abundance, which is mainly produced non-thermally via misalignment. While in this case one should re-assess the WDM bound in the given scenarios, here we refrain from this analysis (which is clearly beyond the scope of this work), and rather apply the lower limit in Eq. (4.18) only when the freeze-in fraction of the total relic abundance exceeds 1%. Typically this happens only for large reheating temperatures $T_R \gg \text{TeV}$ (unless CPon couplings receive extremely large numerical enhancement factors with respect to the natural expectation), so that we can take $g_*(T_R) = 106.75$ and use for concreteness the WDM bound $m_\xi \geq 10$ keV.

Finally we note that if the DM abundance is mainly generated via misalignment, CPons with sufficiently small masses produced via decays and scattering of SM particles could still contribute to dark radiation, which is strongly constrained by BBN and CMB observations.

Using these results of Refs. [143, 144], it is however clear that in our scenario these contributions are very efficiently suppressed by the UV scale $\Lambda \gtrsim 10^{12}$ GeV, which makes the total amount of dark radiation negligible in the phenomenologically relevant regions of parameter space.

5 Concrete realizations

So far the framework we have considered is rather generic. To assess its capability of reproducing the DM abundance while respecting all experimental bounds, we need to specialize our scenario. We consider two realizations, which provide an idea of the stability of our results against variations in the underlying theory.

5.1 Canonical Kähler potential

We start from the simple possibility of a theory with canonical Kähler potential. A general pattern of matrices of Yukawa couplings that automatically verifies the condition in Eq. (2.2) is

$$Y^A(\tau) = \begin{pmatrix} 0 & 0 & c_{A13} \\ 0 & c_{A22} & c_{A23}(\tau)/x_A \\ c_{A31} & c_{A32}(\tau)/x_A & c_{A33}(\tau)/x_A^2 \end{pmatrix} \quad (A = U, D, E), \quad (5.1)$$

where c_{A13} , c_{A22} and c_{A31} are real constants and the τ dependence is carried by the lower-right triangular block. We have included a redundant real parameter x_A , one per each charge sector, that can be eliminated by redefining the 23, 32 and 33 entries. The advantage of this presentation is that when x_A is smaller than one and all constants/functions c_{Aab} are roughly of the same order of magnitude, the singular values of $Y^A(\tau)$ are approximately given by $m_{A1} \approx c_A x_A^2$, $m_{A2} \approx c_A$ and $m_{A3} \approx c_A/x_A^2$, with a proportionality factor $c_A \approx |c_{Aab}|$ of about the same size. This is a good starting point to reproduce the observed hierarchy in the charged fermion sector. The unitary matrices U_{Ac}^T and U_A that diagonalize Y^A via $U_{Ac}^T Y^A U_A = \hat{Y}^A$ have the pattern:

$$U_{Ac}^T \approx U_A \approx \begin{pmatrix} 1 & x_A & x_A^2 \\ x_A & 1 & x_A \\ x_A^2 & x_A & 1 \end{pmatrix}, \quad (5.2)$$

where only the order of magnitude of the entries has been displayed. The coefficients multiplying the off-diagonal terms are indeed ratios of the quantities c_{Aab} , expected to be of order one if these quantities have approximately the same size. It follows that the generic

pattern of the matrix of the CPon couplings, $\hat{g}_A = \langle \hat{Y}_\tau^A \rangle v_A$, evaluated in the basis where $\langle Y^A \rangle$ is diagonal, is

$$\hat{g}_A \approx \frac{c_{A\tau}}{c_A} \begin{pmatrix} m_{A1} & \sqrt{m_{A1}m_{A2}} & \sqrt{m_{A1}m_{A3}} \\ \sqrt{m_{A1}m_{A2}} & m_{A2} & \sqrt{m_{A2}m_{A3}} \\ \sqrt{m_{A1}m_{A3}} & \sqrt{m_{A2}m_{A3}} & m_{A3} \end{pmatrix}, \quad (5.3)$$

where we kept track of the fact that each entry is linearly proportional to a combination of the derivatives of the functions $c_{A23}(\tau)$, $c_{A32}(\tau)$ and $c_{A33}(\tau)$, that we have denoted by a common symbol $c_{A\tau}$. Our estimates depend on the ratio $c_{A\tau}/c_A$, describing the steepness of the functions $c_{A23}(\tau)$, $c_{A32}(\tau)$ and $c_{A33}(\tau)$ evaluated at the minimum of the energy density. Without further knowledge of these functions, we can adopt the simple-minded ansatz

$$c_{A\tau}/c_A \approx 1. \quad (5.4)$$

Our assumptions are probably inadequate to reproduce, at a given energy scale, the precise values of the observed fermion masses and mixing angles. For instance, the c_{Aab} input functions/parameters cannot be all exactly of the same size and they need some amount of tuning to match the experimental precision. Moreover, as we will see in a specific example, the near equality $c_{A\tau}/c_A \approx 1$ can be easily violated by an order of magnitude. Keeping in mind all these caveats, here we will adopt Eqs. (5.3) and (5.4) to assess the allowed parameter space of the model. We also make use of the fermion masses evaluated at the scale of the Z boson mass and listed in Table 1.

m_d (GeV)	$(2.8 \pm 0.3) \times 10^{-3}$
m_s (GeV)	$(54 \pm 3) \times 10^{-3}$
m_b (GeV)	2.85 ± 0.03
m_u (GeV)	$(1.3 \pm 0.5) \times 10^{-3}$
m_c (GeV)	0.63 ± 0.02
m_t (GeV)	171.7 ± 1.6
m_e (GeV)	$(0.486654 \pm 0.000003) \times 10^{-3}$
m_μ (GeV)	$(10.2735 \pm 0.00003) \times 10^{-2}$
m_τ (GeV)	1.74646 ± 0.00002

Table 1: Fermion masses renormalized at the scale m_Z , from Ref. [145].

5.2 A modular-invariant model

As an alternative example, we consider the modular invariant model of Ref. [15], described in Appendix A. Each matter supermultiplet carries a weight k_{Aa} and we consider the simple choice:

$$k_{H_u} = k_{H_d} = 0 \quad k_{Q_a} = k_{U_a^c} = k_{D_a^c} = k_{L_a} = k_{E_a^c} = (-6, 0, 6), \quad (5.5)$$

which enforces the absence of gauge anomalies and guarantees a solution to the strong CP problem. Such a choice determines both the Yukawa couplings and the Kähler potential, in its minimal form. The matrices of Yukawa couplings have entries that are modular forms of weight $k_{A_a^c} + k_{A_b}$:

$$Y^A(\tau) = \begin{pmatrix} 0 & 0 & c_{A13} \\ 0 & c_{A22} & c_{A23}E_6(\tau) \\ c_{A31} & c_{A32}E_6(\tau) & c_{A33}E_6(\tau)^2 + c'_{A33}E_4(\tau)^3 \end{pmatrix} \quad (A = U, D, E),$$

where c_{Aab} and c'_{A33} are real constants, while $E_{4,6}(\tau)$ are the Eisenstein modular forms of weight 4 and 6, see Appendix A. The minimal Kähler metrics $\Omega_A^{c\dagger}\Omega_A^c$ and $\Omega_A^\dagger\Omega_A$ are determined by

$$\Omega_A^c = y^{\frac{-k_{A_a^c}}{2}} \delta_{ab} \quad \Omega_A = y^{\frac{-k_{A_a}}{2}} \delta_{ab} \quad y = -i(\tau - \bar{\tau}). \quad (5.6)$$

Plugging $Y^A(\tau)$ and $\Omega_A^c = \Omega_A$ into the general expressions of Eq. (2.9) we get the mass matrices m_A and couplings g_A of the model. We find

$$m_{Aab} = \langle y^{k_{A_a^c}/2} Y_{ab}^A y^{k_{A_b}/2} \rangle. \quad (5.7)$$

We see that the role of the small parameter x_A discussed in the previous section is played here by $1/y^3$, common to all charged sectors. The couplings g_A read [146]:

$$g_A = \frac{1}{y} \left[\langle y \times y^{k_{A_a^c}/2} Y_{\tau ab}^A y^{k_{A_b}/2} \rangle - i(k_{A_a^c} m_{Aab} + m_{Aab} k_{Ab}) \right]. \quad (5.8)$$

Since g_A only appears in the combination g_A/Λ we will absorb the overall factor $1/y$ by redefining $\Lambda \rightarrow \langle y \rangle \Lambda$. Choosing for convenience $\tau = 1/8 + i$, and fixing the input parameters c_{Aab} and c'_{A33} from a fit to fermion masses and mixing angles (see Appendix A), we can compute the matrices \hat{g}_A in the fermion mass basis. We get:

$$\hat{g}_U = \begin{pmatrix} 0.1189 + 0.085i & 0 & -3.55 + 28.9i \\ 0 & 0 & 0 \\ -88.4 + 42.2i & 0 & -15817 - 11387i \end{pmatrix} \text{ GeV}$$

$$\begin{aligned}
\hat{g}_D &= \begin{pmatrix} 0.168 + 0.531i & 0.195 - 1.74i & -4.59 + 36.3i \\ 0.862 + 2.22i & 0.366 - 7.48i & -8.75 + 156i \\ -4.24 - 0.897i & 11.1 + 7.93i & -226 - 169i \end{pmatrix} \text{ GeV} \\
\hat{g}_E &= \begin{pmatrix} -0.00326 + 0.0232i & 0 & 0.00157 - 0.0111i \\ 0 & 0 & 0 \\ -24.4 + 173i & 0 & 11.7 - 83.1i \end{pmatrix} \text{ GeV}. \tag{5.9}
\end{aligned}$$

Scalar and pseudoscalar couplings are comparable and CP is violated in CPon interactions. These couplings are dominated by the contribution proportional to $Y_{\tau ab}^A$, which is peculiar to this class of models. This is not the case for ALPs, whose couplings to fermions are proportional to the PQ charges (the equivalent of k_A and k_A^c). Moreover, if we compare the couplings of this specific model with those estimated in Eqs. (5.3) and (5.4), we see that the ratio $c_{A\tau}/c_A$ can be larger than one, reaching values between one and two orders of magnitude depending on the specific entries.

5.3 Numerical Results

We now discuss the phenomenology of the CPon in the two explicit realizations detailed above, which we denote by “NAT” (defined by Eq. (5.3) with Eq. (5.4)) and “FIT” (defined by Eq. (5.9)). To specify the CPon couplings to fermions completely, we also have to fix the mixing angle α (cf. Eq. (2.13)). In the following we make the simple choice $\alpha = 0$, other values change the couplings only marginally. We denote the resulting scenarios by “NAT0” and “FIT0”, and display the most relevant couplings in Table 2. The limits discussed in Section 3 from CPon decays (y_{Pee}, y_{See}), flavor constraints ($y_{Sds}, g_{e\mu}$), inverse square law tests and star cooling (y_{SNN}, y_{See}) then only depend on the CPon mass m_ξ and the UV scale Λ , and are displayed in the $m_\xi - \Lambda$ plane in Fig. 1 and 2, showing the excluded regions in gray. Note that in both scenarios limits from HB star cooling and $\mu \rightarrow e\xi$ searches are sub-leading to $K \rightarrow \pi\xi$ constraints. The quantitative difference between the NAT0 and the FIT0 scenario can be easily understood from the numerical values in Table 2, which are smaller in the NAT0 by a factor 10-100, which slightly relaxes the experimental constraints on the parameter space in the $m_\xi - \Lambda$ plane.

The CPon relic abundance instead depends on additional parameters. As discussed in Section 4, we are considering three independent contributions to the DM relic abundance: misalignment, IR-dominated freeze-in and UV-dominated freeze-in. For given couplings \hat{g}_A , the IR-freeze-in contribution depends only on the CPon mass m_ξ and the UV scale Λ , while the UV freeze-in contribution depends also on the reheating temperature T_R (see Eq. (4.17)). The misalignment abundance is independent of fermion couplings, and besides

	$ y_{See} $	$ y_{Pee} $	$ y_{Sds} $	$ y_{SNN} $	$ g_{tt} $	$g_{ct,tc}$	$g_{ut,tu}$
NAT0	3.4×10^{-4}	3.4×10^{-4}	0.027	0.15	2.4×10^2	21	0.94
FIT0	2.3×10^{-3}	1.6×10^{-2}	0.29	8.4	1.9×10^4	0	100

Table 2: Values of phenomenologically relevant couplings in the explicit scenarios in units of GeV. We use the shorthand notation $g_{ij,ji} \equiv \sqrt{|g_{ij}|^2 + |g_{ji}|^2}$.

m_ξ and Λ is set by the initial displacement θ_0 and T_R (see Eq. (4.3) and Eq. (4.5))¹⁶. Thus the total abundance depends on four parameters for a given realization (NAT0 or FIT0 as defined above). In each scenario and fixed θ_0 , we can determine the required value of T_R needed to reproduce the observed DM abundance for given m_ξ and Λ . This value follows from the total contributions to the relic abundance, which in the relevant scenarios are given by the following approximate expressions, where we restrict to the dominant contributions:

$$\Omega_\xi h^2|_{\text{tot}}^{\text{NAT0}} = \left(\frac{m_\xi}{\text{keV}}\right) \left(\frac{10^{12} \text{ GeV}}{\Lambda}\right)^2 \left(5.6 \times 10^{-6} + 0.17 \frac{T_R}{10^8 \text{ GeV}}\right) + \Omega_\xi h^2|_{\text{mis}}, \quad (5.10)$$

$$\Omega_\xi h^2|_{\text{tot}}^{\text{FIT0}} = \left(\frac{m_\xi}{\text{keV}}\right) \left(\frac{10^{12} \text{ GeV}}{\Lambda}\right)^2 \left(3.6 \times 10^{-2} + 0.11 \frac{T_R}{10^4 \text{ GeV}}\right) + \Omega_\xi h^2|_{\text{mis}}, \quad (5.11)$$

where the misalignment contribution is scenario-independent and given by¹⁷

$$\Omega_\xi h^2|_{\text{mis}} = 0.12 \theta_0^2 \begin{cases} \left(\frac{\Lambda}{1.1 \times 10^{11} \text{ GeV}}\right)^2 \left(\frac{m_\xi}{\text{keV}}\right)^{1/2} & T_R \geq 6.7 \times 10^5 \text{ GeV} \sqrt{m_\xi / \text{keV}} \\ \left(\frac{\Lambda}{6.7 \times 10^{11} \text{ GeV}}\right)^2 \left(\frac{T_R}{18 \text{ TeV}}\right) & T_R < 6.7 \times 10^5 \text{ GeV} \sqrt{m_\xi / \text{keV}} \end{cases}. \quad (5.12)$$

In Fig. 1 and 2 we show in blue the contours where the relic abundance can be reproduced for the shown values of T_R , for three representative values of θ_0 and the two scenarios. Dotted contours denote the regions excluded by the Warm DM bound below Eq. (4.18). In the following we discuss the qualitative feature of these contours.

We start with the simplest scenario with vanishing (or very small) initial field values, $\theta_0 = 0$ (Fig. 1). The CPon field sits near the minimum of the energy density, giving a limiting case that we discuss to isolate the feature of pure freeze-in. All DM contour lines follow the scaling $\Lambda \propto m_\xi^{1/2}$. CPon DM is always produced with a large initial velocity and thus is constrained by structure formation (cf. Section 4.3), excluding CPon masses below roughly 10 keV. In order to generate the observed abundance one needs large values of m_ξ and/or small values Λ , most of which are in fact already excluded by a combination of flavor,

¹⁶The dependence on Λ and θ_0 is through the combination $\xi_0 = \Lambda \theta_0$.

¹⁷In case of $T_R < 200 \text{ GeV}$ we only take into account the misalignment contribution, cf. Section 4.2.

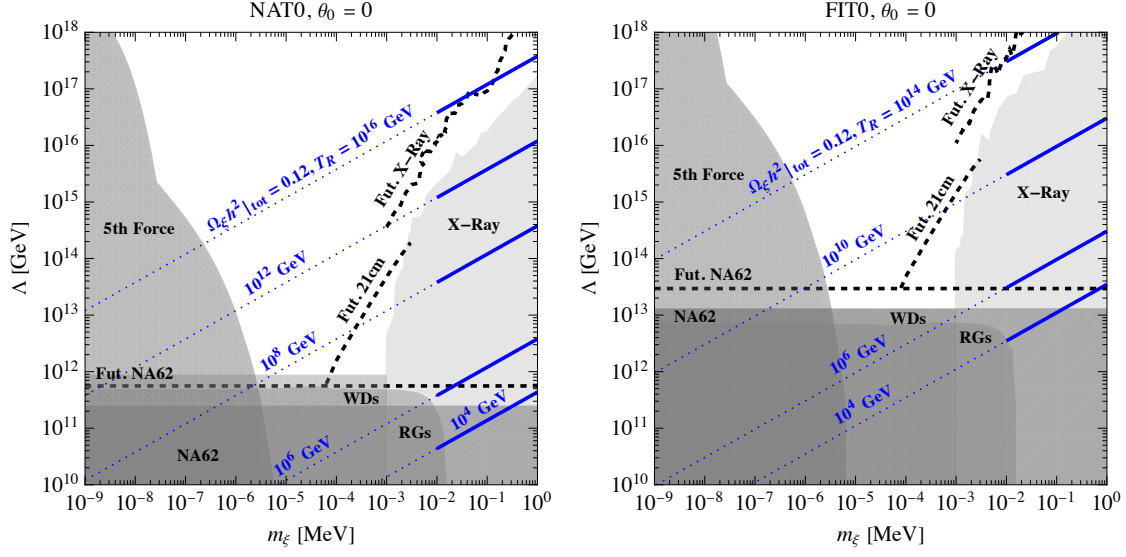


Figure 1: Allowed parameter space for NAT0 (left panel) and FIT0 (right panel) scenarios, for vanishingly small values of the initial misalignment $\theta_0 = 0$. As **gray regions** we show the constraints from Section 3, which are set by X-ray telescopes, inverse square law tests ("5th Force") astrophysics ("RGs" and "WDs") and flavor experiments looking for $K \rightarrow \pi\xi$ decays ("NA62"). We also denote with **black dashed contours** the expected sensitivity using the entire NA62 data set ("Fut. NA62"), the next generation of X-ray telescopes ("Fut. X-ray") and projected limits from the 21-cm power spectrum ("Fut. 21cm"). With **blue contours** we indicated the regions of the parameter space where the observed DM abundance can be reproduced for the shown value of the reheating temperature T_R , with **dotted blue lines** those excluded by the Lyman- α constraints on Warm DM, which require $m_\xi \gtrsim 10$ keV.

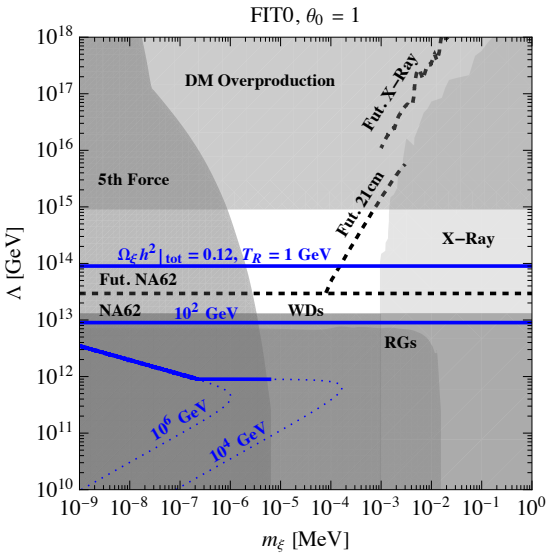


Figure 2: Allowed parameter space for NAT0 (upper panel) and FIT0 (lower panel) scenarios, for indicated values of the initial misalignment $\theta_0 = \{0.01, 1\}$. The **gray regions** and **black dashed contours** are as in Fig. 1. With **blue contours** we indicated the regions of the parameter space where the observed DM abundance can be reproduced for the shown value of the reheating temperature T_R , with **dotted blue lines** by the Lyman- α constraints on Warm DM, which require $m_\xi \gtrsim 10$ keV unless the dominant production is through misalignment (freeze-in contribution less than 1%). The leading contribution to the abundance can be inferred with the scaling of the respective contour: $\Lambda \propto m_\xi^{1/2} T_R^{1/2}$ corresponds to freeze-in, $\Lambda \propto m_\xi^{-1/4} \theta_0^{-1}$ to RD misalignment and $\Lambda \propto T_R^{-1/2} \theta_0^{-1}$ (independent of m_ξ) to EMD misalignment.

astrophysical and X-ray constraints (see lower right contour) in both scenarios. For larger values of Λ the correct abundance can be obtained by increasing T_R , and the parameter space is viable for values roughly above $T_R \approx 10^{12}$ GeV. In this region $\Lambda \propto m_\xi^{1/2} T_R^{1/2}$, so that all parameter space not excluded by other experiments allows to reproduce the observed abundance via UV freeze-in for sufficiently large $T_R < \Lambda$. As can be seen In Fig. 1, the associated parameter space with $T_R > \Lambda$ is excluded by Lyman- α constraints, so we do not explicitly impose this upper bound.

On the other hand we can consider $\theta_0 \approx 1$ (right panel of Fig. 2), where the dominant contribution in the relevant parameter space comes from misalignment, unless for very low values of Λ , which are in fact already excluded by WD and RG cooling and/or flavor constraints. For sufficiently low values of $T_R \lesssim \text{TeV}$ the main contribution to the CPon abundance is due to EMD misalignment. This contribution is then m_ξ -independent, and correspond to the horizontal contour lines in Fig. 2, following $\Lambda \propto T_R^{-1/2} \theta_0^{-1}$. Because of the lower bound on T_R of around 10 MeV from BBN, there is a model-independent upper limit of $\Lambda \lesssim 10^{15} \text{ GeV} / \theta_0$ above which the scenario is excluded by DM overproduction. Larger reheating temperatures thus require lower values of Λ , and temperatures above $T_R \sim 10^4 \text{ GeV}$ ($\sim 10^2 \text{ GeV}$) are excluded for the NAT0 (FIT0) scenario. For reheating temperatures in the allowed window the DM abundance can be reproduced, and there is no WDM bound because DM is sufficiently cold. Although already excluded, it is instructive to consider values of T_R above 10^4 GeV , where the relic abundance can be dominated by UV freeze-in for large values of m_ξ (and low Λ), by EDM misalignment for intermediate values of m_ξ , and by RD misalignment for low values of m_ξ . In the latter region the contour line with the observed relic abundance scale as $\Lambda \propto m_\xi^{-1/4}$, is T_R -independent and not subject to WDM constraints. However for sufficiently large T_R the UV freeze-in contribution starts to become relevant, providing a second solution to the DM abundance with low Λ . While for the chosen value of $\theta_0 = 1$ the RD misalignment contribution is entirely excluded by 5th force experiments, star cooling and/or flavor constraints, this contribution scales as $\Lambda \propto \theta_0^{-1}$, so this case can be made viable for slightly smaller values of θ_0 .

For $\theta_0 = 0.01$ (left panel of Fig. 2) indeed RD misalignment can give the dominant contribution to the observed abundance, without being in conflict with experimental constraints. This is particularly interesting, as in this case the abundance is insensitive to the precise value of T_R in a broad range ($10^6 \text{ GeV} \lesssim T_R \lesssim 10^{14} \text{ GeV}$ for NAT0, and $10^6 \text{ GeV} \lesssim T_R \lesssim 10^9 \text{ GeV}$ for FIT0). Also regions in the parameter space with dominant EMD misalignment are viable, for values of Λ that are larger by factor 100 with respect to the $\theta = 1$, and an excluded region for DM overproduction that shrinks accordingly. Note that regions with dominant UV freeze-in are restricted to $m_\xi \gtrsim 10 \text{ keV}$, and in fact excluded by X-ray constraints on decaying DM. As in Fig. 1 we do not explicitly impose $T_R < \Lambda$ for the freeze-in contribution, as the associated parameter space with $T_R > \Lambda$ in the lower left part of the NAT0 scenario is anyway excluded by Lyman- α constraints.

6 Conclusion

Solutions to the strong CP problem typically require extensions of the Standard Model that include additional spin-zero particles in the spectrum. In the axion solution, the $\bar{\theta}$ parameter is promoted to a pseudoscalar field whose VEV is relaxed to zero by QCD dynamics. This mechanism works independently of the sources of CP violation in the electroweak sector, whose nature remains unexplored. In a wide range of parameter space, the axion is a viable candidate for cold DM, currently under intense experimental search.

A different class of solutions assumes that the theory is invariant under CP, spontaneously broken to deliver the observed CKM phase without affecting $\bar{\theta}$. Such a breaking is achieved by the VEV of a (set of) complex spin-zero field(s), upon which the Yukawa couplings of the theory depend. We have considered this mechanism in the framework of a supersymmetric theory, where the field content of the MSSM is minimally extended to include an extra gauge-singlet chiral supermultiplet. Though supersymmetry is not a mandatory choice, it helps in accommodating the relevant pattern of field-dependent Yukawa matrices, characterized by a constant determinant. The extra supermultiplet has nonrenormalizable interactions with the matter fields of the theory, specified by a scale Λ . Without additional information about the dynamics of the new supermultiplet, we cannot make any precise statement about the low-energy properties of the theory. If the supermultiplet is very heavy, we have little hope of testing this scenario.

There are examples from string theory compactifications where CP is a symmetry of the four-dimensional effective theory and the Yukawa couplings are dynamical quantities depending on a set of moduli fields, some of which can be very light. Here we adopt the working assumption, which we are not able to justify in our bottom-up approach, that one of the two spin-zero components of the extra supermultiplet is light, with a mass m_ξ that we treat as a free parameter. We investigate under which circumstances such a light degree of freedom, the CPon, can act as Dark Matter.

The CPon has CP-violating couplings to ordinary fermions, which are suppressed by the scale Λ and entirely determined by the dynamical Yukawa couplings and by the Kähler potential of the theory. Moreover, these couplings satisfy a sum rule, valid for both canonical and non-canonical Kähler potentials in a large class of scenarios. This sum rule implies that CP-violating and charged lepton contributions to the photon decay rate are suppressed, and the decay amplitude into photons is dominated by the CP-conserving contribution from heavy quarks and light pseudoscalar mesons. The stringent bounds from X-ray telescopes on the CPon lifetime of order $\tau_{\gamma\gamma} \lesssim 10^{29}$ sec, can be evaded if its mass is below 1 MeV (requiring Λ below the Planck scale). The scale Λ is bounded from below (typically to be larger than 10^{12} GeV) by limits on the energy loss in White Dwarfs and Red Giants and by constraints on flavour-violating decays with CPon emission, most notably $K^+ \rightarrow \pi^+ \xi$. Importantly, the CPon mass cannot be arbitrarily small without affecting too much the inverse square law of gravity, with a typical lower bound of $\mathcal{O}(\text{meV})$.

For CPon production in the early universe, we have considered both misalignment

and freeze-in, with a possible period of early matter domination preceding the radiated dominated universe at a temperature T_R . In the allowed parameter space, the CPon can easily saturate the observed Dark Matter abundance for suitable values of T_R , depending on the chosen values of CPon couplings and the initial misalignment.

For a quantitative discussion, we have evaluated the relevant CPon couplings in two representative cases. First, we have provided an order-of-magnitude estimate, based on a typical pattern of Yukawa couplings delivering $\bar{\theta} = 0$. Second, we have computed the CPon coupling constants in a model where the desired Yukawa matrices are ensured by modular invariance. In this case, once the value of the CP-violating VEV has been fixed, all free parameters can be derived from a fit to fermion masses and mixing angles, with little residual uncertainty.

We have analyzed the Dark Matter abundance in both scenarios, see Fig. 1 and 2. Freeze-in is always the dominant mechanism when the initial value of the CPon field is very small. In this case, infrared freeze-in alone falls short to generate the observed relic abundance due to lower bounds on Λ , so that a large reheating temperature is needed to have a sufficiently large contribution from UV freeze-in. Given the present limits on warm Dark Matter and X-ray photons from DM decays, only a little portion of the parameter space is still available, see Fig. 1, partially in the reach of future X-ray missions. Misalignment is the dominant mechanism as soon as the initial field value of the CPon is sufficiently large. For field values of the order of the UV scale, the lower bound on Λ implies an upper bound on the reheating temperature of order $10^{2\div 4}$ GeV, needed for a sufficient dilution of the CPon density in the EMD scenario. For lower initial field values instead the region of viable reheating temperatures opens up, allowing also regions in the parameter space where the dominant contribution to the DM abundance comes from usual RD misalignment. The abundance is then independent of the reheating temperature in a wide range of reheating temperatures between 10^4 GeV $\lesssim T_R \lesssim 10^{9\div 14}$ GeV, for values of Λ around $10^{13\div 14}$ GeV, for the chosen value of the initial misalignment of 0.01Λ .

Though our scenario relies on a strong assumption, the lightness of the CPon, it has the attractive feature of linking three mysteries of fundamental interactions: the flavour puzzle, the origin of CP violation, and the nature of Dark Matter. Moreover, the presently allowed parameter space is compact and will be partially explored by a variety of experimental probes in the near future, such as upcoming X-ray missions, 21cm cosmology, inverse square law tests of gravity, and laboratory searches for rare kaon decays.

Acknowledgements

We thank Joerg Jaeckel, Luca Di Luzio, Hans Peter Nilles, Paolo Panci, Fernando Quevedo, Nicole Righi, Thomas Schwetz and Alessandro Strumia for useful discussions and comments on manuscript. We thank Gabriele Levati for his precious help in the computation of the CPon decay width. The research of F. F. was supported in part by the INFN. F. F. thanks

the KIT in Karlsruhe for hospitality in February 2024, when this project started. This work has received support from the European Union’s Horizon 2020 research and innovation programme under the Marie Skłodowska-Curie grant agreement No 860881-HIDDeN and is partially supported by project B3a and C3b of the DFG-funded Collaborative Research Center TRR257 “Particle Physics Phenomenology after the Higgs Discovery”.

Appendices

A CPon from Modular Invariance

We focus on a supersymmetric modular-invariant [147–149] and CP-invariant [150–152] theory. The Lagrangian \mathcal{L} depends on a set of chiral supermultiplets ϕ comprising one (dimensionless) modulus τ ($\text{Im}\tau > 0$) and the matter superfields ϕ_i of the MSSM. In a compact notation, \mathcal{L} reads:

$$\mathcal{L} = \int d^2\theta d^2\bar{\theta} K(e^{2V}\varphi, \bar{\varphi}) + \left[\int d^2\theta w(\varphi) + h.c. \right] + \left[\frac{1}{16} \int d^2\theta f(\varphi) W^a W^a + h.c. \right], \quad (\text{A.1})$$

where φ collectively denotes all chiral supermultiplets. The Kähler potential K is a real gauge-invariant function. The superpotential $w(\varphi)$ and the gauge kinetic functions $f_\alpha(\varphi)$ ($\alpha = 1, 2, 3$) are gauge-invariant analytic functions. The real and imaginary part of $f_3(\varphi)$ define the strong gauge coupling and the QCD angle ¹⁸:

$$f_3 = \frac{1}{g_S^2} - i \frac{\theta_{\text{QCD}}}{8\pi^2}. \quad (\text{A.2})$$

Modular invariance means that \mathcal{L} remains unchanged under $SL(2, \mathbb{Z})$ transformations:

$$\tau \xrightarrow{\gamma} \gamma\tau = \frac{a\tau + b}{c\tau + d} \quad \phi_i \xrightarrow{\gamma} (c\tau + d)^{-k_i} \phi_i \quad V \xrightarrow{\gamma} V, \quad (\text{A.3})$$

where a, b, c, d are integers obeying $ad - bc = 1$ and k_i , the weights, are integer numbers. Up to modular transformations, under CP the multiplets transform as

$$\tau \xrightarrow{CP} -\bar{\tau} \quad \phi_i \xrightarrow{CP} \bar{\phi}_i \quad V \xrightarrow{CP} \bar{V}. \quad (\text{A.4})$$

The matter superfields ϕ_i are assumed to have either vanishing or negligible VEVs, compared to the VEV of the modulus τ . Since the theory is CP-invariant, the only source

¹⁸We normalize the field strength as $W^a = 2W_B^a$, where W_B^a is according to the definition in Ref. [153]. It follows that $\int d^2\theta W^a W^a = -2F_{\mu\nu}^a F^{a\mu\nu} + 2iF_{\mu\nu}^a \tilde{F}^{a\mu\nu}$, where $\tilde{F}^{a\mu\nu} = 1/2\epsilon^{\mu\nu\rho\sigma} F_{\rho\sigma}^a$. From Eqs. (A.1) and (A.2) we get $1/16 \int d^2\theta f(\varphi) W^a W^a + h.c. = -1/4g_s^2 F_{\mu\nu}^a F^{a\mu\nu} + \theta/32\pi^2 F_{\mu\nu}^a \tilde{F}^{a\mu\nu}$.

of CP violation is the VEV of the modulus τ . Its CP conserving values are along the imaginary τ axis and along the border of the fundamental region $|\Re(\tau)| \leq 1/2$, $|\tau| \geq 1$.

Consistently with modular and CP invariance, we can choose (real positive) constant gauge kinetic functions $f_\alpha(\varphi) = f_{0\alpha}$, such that the QCD angle θ_{QCD} in Eq. (A.2) is zero. We adopt a minimal Kähler potential:

$$K(\phi, \bar{\phi}) = -\Lambda^2 \log y + \sum_i y^{-k_i} \bar{\phi}_i \phi^i \quad y = -i(\tau - \bar{\tau}), \quad (\text{A.5})$$

where Λ is the scale controlling the nonrenormalizable interaction of the modulus. Working in the limit of massless neutrinos, the relevant part of the superpotential w reads

$$w(\varphi) = U_a^c H_u Y_{ab}^U(\tau) Q_b + D_a^c H_d Y_{ab}^D(\tau) Q_b + E_a^c H_d Y_{ab}^E(\tau) L_b + \mu(\tau) H_u H_d. \quad (\text{A.6})$$

Modular invariance requires that the functions $Y_{ab}^{U,D,E}(\tau)$ and $\mu(\tau)$, assumed to be nonsingular, are modular forms of weight $(k_{U_a^c} + k_{Q_b} + k_{H_u})$, $(k_{D_a^c} + k_{Q_b} + k_{H_d})$, $(k_{E_a^c} + k_{L_b} + k_{H_d})$ and $(k_{H_u} + k_{H_d})$, respectively. We choose a basis of modular forms satisfying $Y_{ab}^A(-\bar{\tau}) = \overline{Y_{ab}^A(\tau)}$ and $\mu(-\bar{\tau}) = \overline{\mu(\tau)}$, so that any free parameter in the $w(\varphi)$ is constrained to be real.

In the limit of exact supersymmetry, the physical angle $\bar{\theta}$, invariant under colored fermion chiral rotations, is

$$\bar{\theta} = \theta_{\text{QCD}} + \arg \det \mathcal{M}_U \mathcal{M}_D = \arg \det Y^U(\tau) Y^D(\tau),$$

where $\mathcal{M}_{U,D}$ are the quark mass matrices and we made use of $\theta_{\text{QCD}} = 0$ and the equality $\arg \det \mathcal{M}_U \mathcal{M}_D = \arg \det Y^U(\tau) Y^D(\tau)$, which follows from the fact that the Kähler potential does not affect the phase of the determinant of the mass matrices [50] and the VEVs of Higgs multiplets can be chosen real and positive. The determinant $\det Y^U(\tau) Y^D(\tau)$ is a modular form of weight

$$k_{\text{det}} = \sum_a (k_{U_a^c} + k_{D_a^c} + 2k_{Q_a}) + 3(k_{H_u} + k_{H_d}). \quad (\text{A.7})$$

Modular transformations act as local chiral rotations on canonically normalized fermion fields and the weights of the matter multiplets should ensure the absence of mixed modular-gauge anomalies. A simple solution to the set of conditions guaranteeing anomaly cancellation is [15]

$$k_{H_u} + k_{H_d} = 0 \quad k_{Q_a} = k_{U_a^c} = k_{D_a^c} = k_{L_a} = k_{E_a^c} = (-k, 0, k), \quad (\text{A.8})$$

and we will adopt this choice, which implies $k_{\text{det}} = 0$. The determinant $\det Y^u(\tau) Y^d(\tau)$ is a modular form of vanishing weight, which is a constant required to be real by CP invariance. If this constant is positive, which can be ensured by a proper choice of the free parameters,

the physical angle $\bar{\theta}$ is zero. This result, valid in the limit of unbroken supersymmetry, gets corrected by a tolerable amount if the mechanism of supersymmetry breaking does not introduce new phases and/or new flavour patterns [50, 51]. The determinants of the up, down and electron mass matrices are also all real constants. We remark that the condition for the absence of mixed modular- $U(1)_{QED}^2$, also satisfied by the solution (A.8), reads

$$\sum_a [N_c Q_u^2(k_{Q_a} + k_{U_a^c}) + N_c Q_d^2(k_{Q_a} + k_{D_a^c}) + Q_e^2(k_{L_a} + k_{E_a^c})] + (k_{H_u} + k_{H_d}) = 0. \quad (\text{A.9})$$

Such a condition plays a role in the evaluation of the decay width of the modulus into two photons. In this work, we further specify the choice in Eq. (A.8):

$$k_{H_u} = k_{H_d} = 0 \quad k_{Q_a} = k_{U_a^c} = k_{D_a^c} = k_{L_a} = k_{E_a^c} = (-6, 0, 6). \quad (\text{A.10})$$

As a consequence, $\mu(\tau) = \mu$ is a real constant and the Yukawa couplings are given by

$$Y^A(\tau) = \begin{pmatrix} 0 & 0 & c_{A13} \\ 0 & c_{A22} & c_{A23} E_6(\tau) \\ c_{A31} & c_{A32} E_6(\tau) & c_{A33} E_6(\tau)^2 + c'_{A33} E_4(\tau)^3 \end{pmatrix} \quad (A = U, D, E), \quad (\text{A.11})$$

where c_{Aab} and c'_{A33} are real constants, while $E_{4,6}(\tau)$ are the weight (4, 6) Eisenstein modular forms:

$$E_4(\tau) = 1 + 240 \sum_{n=1}^{\infty} \frac{n^3 \exp(2\pi i n \tau)}{1 - \exp(2\pi i n \tau)} \quad E_6(\tau) = 1 - 504 \sum_{n=1}^{\infty} \frac{n^5 \exp(2\pi i n \tau)}{1 - \exp(2\pi i n \tau)}. \quad (\text{A.12})$$

From Eq. (A.5) we read the minimal Kähler metrics $\Omega_A^{c\dagger} \Omega_A^c$ and $\Omega_A^\dagger \Omega_A$, determined by

$$\Omega_A^c = y^{\frac{-k_{A\bar{a}}}{2}} \delta_{ab} \quad \Omega_A = y^{\frac{-k_{Aa}}{2}} \delta_{ab}. \quad (\text{A.13})$$

Plugging $Y^A(\tau)$ and $\Omega_A^c = \Omega_A$ into the general expressions of Eq. (2.9) we get the mass matrices m_A and couplings g_A of the model. We find

$$m_A(\tau) = \begin{pmatrix} 0 & 0 & c_{A13} \\ 0 & c_{A22} & y^3 c_{A23} E_6(\tau) \\ c_{A31} & y^3 c_{A32} E_6(\tau) & y^6 [c_{A33} E_6(\tau)^2 + c'_{A33} E_4(\tau)^3] \end{pmatrix} v_A, \quad (\text{A.14})$$

where $v_U = v \sin \beta$ and $v_D = v_E = v \cos \beta$, $v \approx 174$ GeV and τ is evaluated at its VEV. We see that the role of the small parameter x_A discussed in Section 5 is played here by

$1/y^3$, common to all charged sectors. In this class of models $\text{Im}(\tau) \geq \sqrt{3}/2$, and we have $1/y^3 < 0.2$. The couplings g_A read:

$$g_{Aab} = \frac{1}{y} \left[\langle y \times y^{k_{A_a^c}/2} Y_{\tau ab}^A y^{k_{A_b}/2} \rangle - i(k_{A_a^c} m_{Aab} + m_{Aab} k_{A_b}) \right]. \quad (\text{A.15})$$

Since g_A only appears in the combination g_A/Λ we will absorb the overall factor $1/y$ by redefining $\Lambda \rightarrow \langle y \rangle \Lambda$. There are more free parameters than observables. We reduce the number of free parameters by choosing:

$$\tau = 1/8 + i.$$

Working in the vicinity of the imaginary unit has proved useful [154–158] in model building. Moreover, we have simple approximate expressions for the quantities of interest by making an expansion in the small parameter $x = 1/y^3 = 0.125$. In addition, we choose:

$$\begin{aligned} c_{U23} = c_{U32} = c_{E23} = c_{E32} &= 0 & \tan \beta &= 10 \\ \arg[c_{U33} E_6(\tau)^2 + c'_{U33} E_4(\tau)^3] &= \arg[c_{D33} E_6(\tau)^2 + c'_{D33} E_4(\tau)^3] & \text{at } \tau &= 1/8 + i. \end{aligned}$$

We are left with a total of 16 real parameters (vs. 13 observables), to be determined by maximizing the agreement with fermion masses, mixing angles and CKM phase. The experimental data and their errors, renormalized at the scale m_Z and taken from Ref. [145], are collected in Table 4. We show the best fit values of c_{Aab} , c'_{Aab} in Table 3. In Table

A	c_{A13}	c_{A22}	c_{A23}	c_{A31}	c_{A32}	c_{A33}	c'_{A33}
D	1.063	0.541	−1.278	0.143	−0.109	−1.194	−0.395
U	0.148	0.362	0	0.498	0	−7.186	−2.379
E	0.00312	0.593	0	9.09	0	0.756	0.192

Table 3: Coefficients c_{Aab} and c'_{Aab} in units 0.01. We choose $v_U = 173.3$ GeV and $v_D = 17.3$ GeV.

4 we display the model predictions evaluated at the best-fit point and we compare them with the experimental values. The agreement in the lepton sector is very good, while in the quark sector is decent, with some discrepancies due to the use of approximate theoretical expressions for the quantities of interest. Evaluating the modulus coupling constants in the basis where the mass matrices are diagonal we get we find

$$\hat{g}_U = \begin{pmatrix} 0.1189 + 0.085i & 0 & -3.55 + 28.9i \\ 0 & 0 & 0 \\ -88.4 + 42.2i & 0 & -15817 - 11387i \end{pmatrix} \text{ GeV}$$

	Experiment	Model
m_d (GeV)	$(2.8 \pm 0.3) \times 10^{-3}$	2.6×10^{-3}
m_s (GeV)	$(54 \pm 3) \times 10^{-2}$	50×10^{-3}
m_b (GeV)	2.85 ± 0.03	3.19
m_u (GeV)	$(1.3 \pm 0.5) \times 10^{-3}$	1.3×10^{-3}
m_c (GeV)	0.63 ± 0.02	0.63
m_t (GeV)	171.7 ± 1.6	171.7
$\sin \theta_{12}$	0.22540 ± 0.00070	0.213
$\sin \theta_{23}$	0.0420 ± 0.0006	0.045
$\sin \theta_{13}$	0.00364 ± 0.00013	0.0019
$\sin \delta$	0.93 ± 0.02	0.88
m_e (GeV)	$(0.486654 \pm 0.000003) \times 10^{-3}$	0.486653×10^{-3}
m_μ (GeV)	$(10.2735 \pm 0.00003) \times 10^{-2}$	10.2735×10^{-2}
m_τ (GeV)	1.74646 ± 0.00002	1.74645

Table 4: Left column: fermion masses, mixing angles, and CKM phase, renormalized at the scale m_Z , from Ref. [145]. Right column: model predictions from $\tau = 1/8 + i$, $\tan \beta = 10$ and the input parameters of Table 3.

$$\begin{aligned}
\hat{g}_D &= \begin{pmatrix} 0.168 + 0.531i & 0.195 - 1.74i & -4.59 + 36.3i \\ 0.862 + 2.22i & 0.366 - 7.48i & -8.75 + 156i \\ -4.24 - 0.897i & 11.1 + 7.93i & -226 - 169i \end{pmatrix} \text{ GeV} \\
\hat{g}_E &= \begin{pmatrix} -0.00326 + 0.0232i & 0 & 0.00157 - 0.0111i \\ 0 & 0 & 0 \\ -24.4 + 173i & 0 & 11.7 - 83.1i \end{pmatrix} \text{ GeV}.
\end{aligned} \tag{A.16}$$

References

- [1] M. Cirelli, A. Strumia, and J. Zupan, *Dark Matter*, [arXiv:2406.01705](#).
- [2] S. Weinberg, *A New Light Boson?*, Phys. Rev. Lett. **40** (1978) 223–226.
- [3] F. Wilczek, *Problem of Strong P and T Invariance in the Presence of Instantons*, Phys. Rev. Lett. **40** (1978) 279–282.
- [4] R. D. Peccei and H. R. Quinn, *CP Conservation in the Presence of Instantons*, Phys. Rev. Lett. **38** (1977) 1440–1443.
- [5] J. Preskill, M. B. Wise, and F. Wilczek, *Cosmology of the Invisible Axion*, Phys. Lett. B **120** (1983) 127–132.
- [6] L. F. Abbott and P. Sikivie, *A Cosmological Bound on the Invisible Axion*, Phys. Lett. B **120** (1983) 133–136.
- [7] M. Dine and W. Fischler, *The Not So Harmless Axion*, Phys. Lett. B **120** (1983) 137–141.
- [8] L. Di Luzio, M. Giannotti, E. Nardi, and L. Visinelli, *The landscape of QCD axion models*, Phys. Rept. **870** (2020) 1–117, [[arXiv:2003.01100](#)].
- [9] M. Kamionkowski and J. March-Russell, *Planck scale physics and the Peccei-Quinn mechanism*, Phys. Lett. B **282** (1992) 137–141, [[hep-th/9202003](#)].
- [10] A. Davidson and K. C. Wali, *MINIMAL FLAVOR UNIFICATION VIA MULTIGENERATIONAL PECCEI-QUINN SYMMETRY*, Phys. Rev. Lett. **48** (1982) 11.
- [11] F. Wilczek, *Axions and Family Symmetry Breaking*, Phys. Rev. Lett. **49** (1982) 1549–1552.
- [12] Z. G. Berezhiani and M. Y. Khlopov, *Cosmology of Spontaneously Broken Gauge Family Symmetry*, Z. Phys. C **49** (1991) 73–78.
- [13] Y. Ema, K. Hamaguchi, T. Moroi, and K. Nakayama, *Flaxion: a minimal extension to solve puzzles in the standard model*, JHEP **01** (2017) 096, [[arXiv:1612.05492](#)].
- [14] L. Calibbi, F. Goertz, D. Redigolo, R. Ziegler, and J. Zupan, *Minimal axion model from flavor*, Phys. Rev. D **95** (2017), no. 9 095009, [[arXiv:1612.08040](#)].
- [15] F. Feruglio, A. Strumia, and A. Titov, *Modular invariance and the QCD angle*, JHEP **07** (2023) 027, [[arXiv:2305.08908](#)].

- [16] F. Feruglio, M. Parriciatu, A. Strumia, and A. Titov, *Solving the strong CP problem without axions*, JHEP **08** (2024) 214, [[arXiv:2406.01689](#)].
- [17] A. E. Nelson, *Naturally Weak CP Violation*, Phys. Lett. B **136** (1984) 387–391.
- [18] S. M. Barr, *Solving the Strong CP Problem Without the Peccei-Quinn Symmetry*, Phys. Rev. Lett. **53** (1984) 329.
- [19] H. Georgi, *A Model of Soft CP Violation*, Hadronic J. **1** (1978) 155.
- [20] L. Hall, C. A. Manzari, and B. Noether, *Strong CP and Flavor in Multi-Higgs Theories*, [arXiv:2407.14585](#).
- [21] R. Ferro-Hernandez, S. Morisi, and E. Peinado, *Axionless strong CP problem solution: the spontaneous CP violation case*, [arXiv:2407.18161](#).
- [22] S. Antusch, M. Holthausen, M. A. Schmidt, and M. Spinrath, *Solving the Strong CP Problem with Discrete Symmetries and the Right Unitarity Triangle*, Nucl. Phys. B **877** (2013) 752–771, [[arXiv:1307.0710](#)].
- [23] L. Vecchi, *Spontaneous CP violation and the strong CP problem*, JHEP **04** (2017) 149, [[arXiv:1412.3805](#)].
- [24] M. Dine and P. Draper, *Challenges for the Nelson-Barr Mechanism*, JHEP **08** (2015) 132, [[arXiv:1506.05433](#)].
- [25] J. Schwichtenberg, P. Tremper, and R. Ziegler, *A grand-unified Nelson–Barr model*, Eur. Phys. J. C **78** (2018), no. 11 910, [[arXiv:1802.08109](#)].
- [26] A. Valenti and L. Vecchi, *The CKM phase and $\bar{\theta}$ in Nelson-Barr models*, JHEP **07** (2021), no. 203 203, [[arXiv:2105.09122](#)].
- [27] A. Valenti and L. Vecchi, *Super-soft CP violation*, JHEP **07** (2021), no. 152 152, [[arXiv:2106.09108](#)].
- [28] S. Nakagawa, Y. Nakai, and Y. Wang, *Spontaneous CP violation in supersymmetric QCD*, JHEP **09** (2024) 105, [[arXiv:2406.01260](#)].
- [29] L. J. Hall, K. Jedamzik, J. March-Russell, and S. M. West, *Freeze-In Production of FIMP Dark Matter*, JHEP **03** (2010) 080, [[arXiv:0911.1120](#)].
- [30] P. Panci, D. Redigolo, T. Schwetz, and R. Ziegler, *Axion dark matter from lepton flavor-violating decays*, Phys. Lett. B **841** (2023) 137919, [[arXiv:2209.03371](#)].
- [31] M. Aghaie, G. Armando, A. Conaci, et al., *Axion dark matter from heavy quarks*, Phys. Lett. B **856** (2024) 138923, [[arXiv:2404.12199](#)].

- [32] S. T. Petcov and M. Tanimoto, *A_4 modular invariance and the strong CP problem*, Eur. Phys. J. C **84** (2024), no. 9 914, [[arXiv:2404.00858](#)].
- [33] J. T. Penedo and S. T. Petcov, *Finite modular symmetries and the strong CP problem*, JHEP **10** (2024) 172, [[arXiv:2404.08032](#)].
- [34] M. Cvetič, A. Font, L. E. Ibanez, D. Lust, and F. Quevedo, *Target space duality, supersymmetry breaking and the stability of classical string vacua*, Nucl. Phys. B **361** (1991) 194–232.
- [35] K. Ishiguro, T. Kobayashi, and H. Otsuka, *Spontaneous CP violation and symplectic modular symmetry in Calabi-Yau compactifications*, Nucl. Phys. B **973** (2021) 115598, [[arXiv:2010.10782](#)].
- [36] P. P. Novichkov, J. T. Penedo, and S. T. Petcov, *Modular flavour symmetries and modulus stabilisation*, JHEP **03** (2022) 149, [[arXiv:2201.02020](#)].
- [37] J. M. Leedom, N. Righi, and A. Westphal, *Heterotic de Sitter beyond modular symmetry*, JHEP **02** (2023) 209, [[arXiv:2212.03876](#)].
- [38] T. Higaki, T. Kobayashi, K. Nasu, and H. Otsuka, *Spontaneous CP violation and partially broken modular flavor symmetries*, JHEP **09** (2024) 024, [[arXiv:2405.18813](#)].
- [39] T. Banks and M. Dine, *Couplings and scales in strongly coupled heterotic string theory*, Nucl. Phys. B **479** (1996) 173–196, [[hep-th/9605136](#)].
- [40] K. Choi, E. J. Chun, and H. B. Kim, *Cosmology of light moduli*, Phys. Rev. D **58** (1998) 046003, [[hep-ph/9801280](#)].
- [41] M. Cicoli, M. Goodsell, and A. Ringwald, *The type IIB string axiverse and its low-energy phenomenology*, JHEP **10** (2012) 146, [[arXiv:1206.0819](#)].
- [42] M. Cicoli, V. Guidetti, N. Righi, and A. Westphal, *Fuzzy Dark Matter candidates from string theory*, JHEP **05** (2022) 107, [[arXiv:2110.02964](#)].
- [43] M. Cicoli, J. P. Conlon, A. Maharana, et al., *String cosmology: From the early universe to today*, Phys. Rept. **1059** (2024) 1–155, [[arXiv:2303.04819](#)].
- [44] S. Funakoshi, J. Kawamura, T. Kobayashi, K. Nasu, and H. Otsuka, *Moduli stabilization and light axion by Siegel modular forms*, [arXiv:2409.19261](#).
- [45] T. Higaki, J. Kawamura, and T. Kobayashi, *Finite modular axion and radiative moduli stabilization*, JHEP **04** (2024) 147, [[arXiv:2402.02071](#)].

- [46] A. Baur, M.-C. Chen, V. Knapp-Perez, and S. Ramos-Sanchez, *Modular flavored dark matter*, JHEP **12** (2024) 091, [[arXiv:2409.02178](#)].
- [47] D. Chowdhury, E. Dudas, M. Dutra, and Y. Mambrini, *Moduli Portal Dark Matter*, Phys. Rev. D **99** (2019), no. 9 095028, [[arXiv:1811.01947](#)].
- [48] M. Dine, G. Perez, W. Ratzinger, and I. Savoray, *Nelson-Barr ultralight dark matter*, Phys. Rev. D **111** (2025), no. 1 015049, [[arXiv:2405.06744](#)].
- [49] B. Grzadkowski and D. Huang, *Spontaneous CP-Violating Electroweak Baryogenesis and Dark Matter from a Complex Singlet Scalar*, JHEP **08** (2018) 135, [[arXiv:1807.06987](#)].
- [50] G. Hiller and M. Schmaltz, *Solving the Strong CP Problem with Supersymmetry*, Phys. Lett. B **514** (2001) 263–268, [[hep-ph/0105254](#)].
- [51] G. Hiller and M. Schmaltz, *Strong Weak CP Hierarchy from Nonrenormalization Theorems*, Phys. Rev. D **65** (2002) 096009, [[hep-ph/0201251](#)].
- [52] J. R. Ellis and M. K. Gaillard, *Strong and Weak CP Violation*, Nucl. Phys. B **150** (1979) 141–162.
- [53] I. B. Khriplovich, *Quark Electric Dipole Moment and Induced θ Term in the Kobayashi-Maskawa Model*, Phys. Lett. B **173** (1986) 193–196.
- [54] A. Kusenko, M. Loewenstein, and T. T. Yanagida, *Moduli dark matter and the search for its decay line using Suzaku X-ray telescope*, Phys. Rev. D **87** (2013), no. 4 043508, [[arXiv:1209.6403](#)].
- [55] F. Quevedo, *Local String Models and Moduli Stabilisation*, Mod. Phys. Lett. A **30** (2015), no. 07 1530004, [[arXiv:1404.5151](#)].
- [56] T. R. Slatyer and C.-L. Wu, *General Constraints on Dark Matter Decay from the Cosmic Microwave Background*, Phys. Rev. D **95** (2017), no. 2 023010, [[arXiv:1610.06933](#)].
- [57] A. Djouadi, *The Anatomy of electro-weak symmetry breaking. I: The Higgs boson in the standard model*, Phys. Rept. **457** (2008) 1–216, [[hep-ph/0503172](#)].
- [58] A. Djouadi, *The Anatomy of electro-weak symmetry breaking. II. The Higgs bosons in the minimal supersymmetric model*, Phys. Rept. **459** (2008) 1–241, [[hep-ph/0503173](#)].
- [59] R. Franceschini, G. F. Giudice, J. F. Kamenik, et al., *What is the $\gamma\gamma$ resonance at 750 GeV?*, JHEP **03** (2016) 144, [[arXiv:1512.04933](#)].

- [60] F. Takahashi, M. Yamada, and W. Yin, *XENON1T Excess from Anomaly-Free Axionlike Dark Matter and Its Implications for Stellar Cooling Anomaly*, Phys. Rev. Lett. **125** (2020), no. 16 161801, [[arXiv:2006.10035](#)].
- [61] C. Han, M. L. López-Ibáñez, A. Melis, O. Vives, and J. M. Yang, *Anomaly-free leptophilic axionlike particle and its flavor violating tests*, Phys. Rev. D **103** (2021), no. 3 035028, [[arXiv:2007.08834](#)].
- [62] C. Han, M. L. López-Ibáñez, A. Melis, O. Vives, and J. M. Yang, *Anomaly-free ALP from non-Abelian flavor symmetry*, JHEP **08** (2022) 306, [[arXiv:2203.16376](#)].
- [63] K. Sakurai and F. Takahashi, *Anomaly-free axion dark matter in three Higgs doublet model and its phenomenological implications*, JHEP **07** (2022) 124, [[arXiv:2203.17212](#)]. [Erratum: JHEP 09, 132 (2023)].
- [64] H. Leutwyler and M. A. Shifman, *GOLDSTONE BOSONS GENERATE PECULIAR CONFORMAL ANOMALIES*, Phys. Lett. B **221** (1989) 384–388.
- [65] V. V. Flambaum and I. B. Samsonov, *Limits on scalar dark matter interactions with particles other than the photon via loop corrections to the scalar-photon coupling*, Phys. Rev. D **110** (2024), no. 7 075044, [[arXiv:2403.02685](#)].
- [66] F. Arias-Aragón, F. D’Eramo, R. Z. Ferreira, L. Merlo, and A. Notari, *Production of Thermal Axions across the ElectroWeak Phase Transition*, JCAP **03** (2021) 090, [[arXiv:2012.04736](#)].
- [67] B. Bolliet, J. Chluba, and R. Battye, *Spectral distortion constraints on photon injection from low-mass decaying particles*, Mon. Not. Roy. Astron. Soc. **507** (2021), no. 3 3148–3178, [[arXiv:2012.07292](#)].
- [68] M. Cirelli, E. Moulin, P. Panci, P. D. Serpico, and A. Viana, *Gamma ray constraints on Decaying Dark Matter*, Phys. Rev. D **86** (2012) 083506, [[arXiv:1205.5283](#)].
- [69] R. Laha, J. B. Muñoz, and T. R. Slatyer, *INTEGRAL constraints on primordial black holes and particle dark matter*, Phys. Rev. D **101** (2020), no. 12 123514, [[arXiv:2004.00627](#)].
- [70] C. R. Watson, Z.-Y. Li, and N. K. Polley, *Constraining Sterile Neutrino Warm Dark Matter with Chandra Observations of the Andromeda Galaxy*, JCAP **03** (2012) 018, [[arXiv:1111.4217](#)].
- [71] S. Horiuchi, P. J. Humphrey, J. Onorbe, et al., *Sterile neutrino dark matter bounds from galaxies of the Local Group*, Phys. Rev. D **89** (2014), no. 2 025017, [[arXiv:1311.0282](#)].

- [72] J. W. Foster, S. Kumar, B. R. Safdi, and Y. Soreq, *Dark Grand Unification in the axiverse: decaying axion dark matter and spontaneous baryogenesis*, JHEP **12** (2022) 119, [[arXiv:2208.10504](#)].
- [73] K. Perez, K. C. Y. Ng, J. F. Beacom, et al., *Almost closing the ν MSM sterile neutrino dark matter window with NuSTAR*, Phys. Rev. D **95** (2017), no. 12 123002, [[arXiv:1609.00667](#)].
- [74] B. M. Roach, K. C. Y. Ng, K. Perez, et al., *NuSTAR Tests of Sterile-Neutrino Dark Matter: New Galactic Bulge Observations and Combined Impact*, Phys. Rev. D **101** (2020), no. 10 103011, [[arXiv:1908.09037](#)].
- [75] K. C. Y. Ng, B. M. Roach, K. Perez, et al., *New Constraints on Sterile Neutrino Dark Matter from NuSTAR M31 Observations*, Phys. Rev. D **99** (2019) 083005, [[arXiv:1901.01262](#)].
- [76] B. M. Roach, S. Rossland, K. C. Y. Ng, et al., *Long-exposure NuSTAR constraints on decaying dark matter in the Galactic halo*, Phys. Rev. D **107** (2023), no. 2 023009, [[arXiv:2207.04572](#)].
- [77] A. Coogan et al., *Hunting for dark matter and new physics with GECCO*, Phys. Rev. D **107** (2023), no. 2 023022, [[arXiv:2101.10370](#)].
- [78] C. Thorpe-Morgan, D. Malyshev, A. Santangelo, et al., *THESEUS insights into axionlike particles, dark photon, and sterile neutrino dark matter*, Phys. Rev. D **102** (2020), no. 12 123003, [[arXiv:2008.08306](#)].
- [79] A. Neronov and D. Malyshev, *Toward a full test of the ν MSM sterile neutrino dark matter model with Athena*, Phys. Rev. D **93** (2016), no. 6 063518, [[arXiv:1509.02758](#)].
- [80] A. Dekker, E. Peerbooms, F. Zimmer, K. C. Y. Ng, and S. Ando, *Searches for sterile neutrinos and axionlike particles from the Galactic halo with eROSITA*, Phys. Rev. D **104** (2021), no. 2 023021, [[arXiv:2103.13241](#)].
- [81] S. Ando et al., *Decaying dark matter in dwarf spheroidal galaxies: Prospects for x-ray and gamma-ray telescopes*, Phys. Rev. D **104** (2021), no. 2 023022, [[arXiv:2103.13242](#)].
- [82] E. Todarello, M. Regis, J. Reynoso-Cordova, et al., *Robust bounds on ALP dark matter from dwarf spheroidal galaxies in the optical MUSE-Faint survey*, JCAP **05** (2024) 043, [[arXiv:2307.07403](#)].
- [83] E. Todarello and M. Regis, *Bounds on Axions-Like Particles Shining in the Ultra-Violet*, [arXiv:2412.02543](#).

- [84] Y. Sun, J. W. Foster, H. Liu, J. B. Muñoz, and T. R. Slatyer, *Inhomogeneous energy injection in the 21-cm power spectrum: Sensitivity to dark matter decay*, Phys. Rev. D **111** (2025), no. 4 043015, [[arXiv:2312.11608](#)].
- [85] R. Ziegler, *Flavor Probes of Axion Dark Matter*, PoS DISCRETE2022 (2024) 086, [[arXiv:2303.13353](#)].
- [86] **NA62** Collaboration, E. Cortina Gil et al., *Measurement of the very rare $K^+ \rightarrow \pi^+ \nu \bar{\nu}$ decay*, JHEP **06** (2021) 093, [[arXiv:2103.15389](#)].
- [87] E. Goudzovski et al., *New physics searches at kaon and hyperon factories*, Rept. Prog. Phys. **86** (2023), no. 1 016201, [[arXiv:2201.07805](#)].
- [88] N. Carrasco, P. Lami, V. Lubicz, et al., *$K \rightarrow \pi$ semileptonic form factors with $N_f = 2 + 1 + 1$ twisted mass fermions*, Phys. Rev. D **93** (2016), no. 11 114512, [[arXiv:1602.04113](#)].
- [89] **Fermilab Lattice, MILC** Collaboration, A. Bazavov et al., *$|V_{us}|$ from $K_{\ell 3}$ decay and four-flavor lattice QCD*, Phys. Rev. D **99** (2019), no. 11 114509, [[arXiv:1809.02827](#)].
- [90] **Flavour Lattice Averaging Group (FLAG)** Collaboration, Y. Aoki et al., *FLAG Review 2021*, Eur. Phys. J. C **82** (2022), no. 10 869, [[arXiv:2111.09849](#)].
- [91] J. Martin Camalich, M. Pospelov, P. N. H. Vuong, R. Ziegler, and J. Zupan, *Quark Flavor Phenomenology of the QCD Axion*, Phys. Rev. D **102** (2020), no. 1 015023, [[arXiv:2002.04623](#)].
- [92] L. Calibbi, D. Redigolo, R. Ziegler, and J. Zupan, *Looking forward to lepton-flavor-violating ALPs*, JHEP **09** (2021) 173, [[arXiv:2006.04795](#)].
- [93] A. Jodidio et al., *Search for Right-Handed Currents in Muon Decay*, Phys. Rev. D **34** (1986) 1967. [Erratum: Phys.Rev.D 37, 237 (1988)].
- [94] **TWIST** Collaboration, R. Bayes et al., *Search for two body muon decay signals*, Phys. Rev. D **91** (2015), no. 5 052020, [[arXiv:1409.0638](#)].
- [95] Y. Jho, S. Knapen, and D. Redigolo, *Lepton-flavor violating axions at MEG II*, JHEP **10** (2022) 029, [[arXiv:2203.11222](#)].
- [96] S. Knapen, K. Langhoff, T. Opferkuch, and D. Redigolo, *A Robust Search for Lepton Flavour Violating Axions at Mu3e*, [arXiv:2311.17915](#).
- [97] R. J. Hill, R. Plestid, and J. Zupan, *Searching for new physics at $\mu \rightarrow e$ facilities with μ^+ and π^+ decays at rest*, Phys. Rev. D **109** (2024), no. 3 035025, [[arXiv:2310.00043](#)].

- [98] **Belle-II** Collaboration, I. Adachi et al., *Search for Lepton-Flavor-Violating τ Decays to a Lepton and an Invisible Boson at Belle II*, Phys. Rev. Lett. **130** (2023), no. 18 181803, [[arXiv:2212.03634](#)].
- [99] **Belle-II** Collaboration, I. Adachi et al., *Evidence for $B^+ \rightarrow K^+ \nu \nu$ decays*, Phys. Rev. D **109** (2024), no. 11 112006, [[arXiv:2311.14647](#)].
- [100] C. A. J. O’Hare and E. Vitagliano, *Cornering the axion with CP-violating interactions*, Phys. Rev. D **102** (2020), no. 11 115026, [[arXiv:2010.03889](#)].
- [101] Y. J. Chen, W. K. Tham, D. E. Krause, et al., *Stronger Limits on Hypothetical Yukawa Interactions in the 30–8000 nm Range*, Phys. Rev. Lett. **116** (2016), no. 22 221102, [[arXiv:1410.7267](#)].
- [102] D. J. Kapner, T. S. Cook, E. G. Adelberger, et al., *Tests of the gravitational inverse-square law below the dark-energy length scale*, Phys. Rev. Lett. **98** (2007) 021101, [[hep-ph/0611184](#)].
- [103] J. G. Lee, E. G. Adelberger, T. S. Cook, S. M. Fleischer, and B. R. Heckel, *New Test of the Gravitational $1/r^2$ Law at Separations down to 52 μm* , Phys. Rev. Lett. **124** (2020), no. 10 101101, [[arXiv:2002.11761](#)].
- [104] S.-Q. Yang, B.-F. Zhan, Q.-L. Wang, et al., *Test of the Gravitational Inverse Square Law at Millimeter Ranges*, Phys. Rev. Lett. **108** (2012) 081101.
- [105] W.-H. Tan et al., *Improvement for Testing the Gravitational Inverse-Square Law at the Submillimeter Range*, Phys. Rev. Lett. **124** (2020), no. 5 051301.
- [106] L.-C. Tu, S.-G. Guan, J. Luo, C.-G. Shao, and L.-X. Liu, *Null Test of Newtonian Inverse-Square Law at Submillimeter Range with a Dual-Modulation Torsion Pendulum*, Phys. Rev. Lett. **98** (2007) 201101.
- [107] W.-H. Tan, S.-Q. Yang, C.-G. Shao, et al., *New Test of the Gravitational Inverse-Square Law at the Submillimeter Range with Dual Modulation and Compensation*, Phys. Rev. Lett. **116** (2016), no. 13 131101.
- [108] M. A. Shifman, A. I. Vainshtein, and V. I. Zakharov, *Remarks on Higgs Boson Interactions with Nucleons*, Phys. Lett. B **78** (1978) 443–446.
- [109] H.-Y. Cheng and C.-W. Chiang, *Revisiting Scalar and Pseudoscalar Couplings with Nucleons*, JHEP **07** (2012) 009, [[arXiv:1202.1292](#)].
- [110] G. G. Raffelt, *Stars as laboratories for fundamental physics: The astrophysics of neutrinos, axions, and other weakly interacting particles*. 5, 1996.

- [111] S. Bottaro, A. Caputo, G. Raffelt, and E. Vitagliano, *Stellar limits on scalars from electron-nucleus bremsstrahlung*, JCAP **07** (2023) 071, [[arXiv:2303.00778](#)].
- [112] Y. Yamamoto and K. Yoshioka, *Stellar cooling limits on light scalar boson revisited*, Phys. Lett. B **843** (2023) 138027, [[arXiv:2303.03123](#)].
- [113] J. A. Grifols and E. Masso, *Constraints on Finite Range Baryonic and Leptonic Forces From Stellar Evolution*, Phys. Lett. B **173** (1986) 237–240.
- [114] E. Hardy and R. Lasenby, *Stellar cooling bounds on new light particles: plasma mixing effects*, JHEP **02** (2017) 033, [[arXiv:1611.05852](#)].
- [115] **CAST** Collaboration, V. Anastassopoulos et al., *New CAST Limit on the Axion-Photon Interaction*, Nature Phys. **13** (2017) 584–590, [[arXiv:1705.02290](#)].
- [116] J. R. Ellis, S. Ferrara, and D. V. Nanopoulos, *CP Violation and Supersymmetry*, Phys. Lett. B **114** (1982) 231–234.
- [117] G. F. Giudice and R. Rattazzi, *Theories with gauge mediated supersymmetry breaking*, Phys. Rept. **322** (1999) 419–499, [[hep-ph/9801271](#)].
- [118] L. Randall and R. Sundrum, *Out of this world supersymmetry breaking*, Nucl. Phys. B **557** (1999) 79–118, [[hep-th/9810155](#)].
- [119] G. F. Giudice, M. A. Luty, H. Murayama, and R. Rattazzi, *Gaugino mass without singlets*, JHEP **12** (1998) 027, [[hep-ph/9810442](#)].
- [120] R. Rattazzi, A. Strumia, and J. D. Wells, *Phenomenology of deflected anomaly mediation*, Nucl. Phys. B **576** (2000) 3–28, [[hep-ph/9912390](#)].
- [121] V. Enguita, B. Gavela, B. Grinstein, and P. Quilez, *ALP contribution to the strong CP problem*, Phys. Rev. D **110** (2024), no. 1 015024, [[arXiv:2403.12133](#)].
- [122] M. Pospelov and A. Ritz, *Theta vacua, QCD sum rules, and the neutron electric dipole moment*, Nucl. Phys. B **573** (2000) 177–200, [[hep-ph/9908508](#)].
- [123] C. Abel et al., *Measurement of the Permanent Electric Dipole Moment of the Neutron*, Phys. Rev. Lett. **124** (2020), no. 8 081803, [[arXiv:2001.11966](#)].
- [124] P. Arias, D. Cadamuro, M. Goodsell, et al., *WISPy Cold Dark Matter*, JCAP **06** (2012) 013, [[arXiv:1201.5902](#)].
- [125] N. Blinov, M. J. Dolan, P. Draper, and J. Kozaczuk, *Dark matter targets for axionlike particle searches*, Phys. Rev. D **100** (2019), no. 1 015049, [[arXiv:1905.06952](#)].

- [126] C. A. J. O’Hare, *Cosmology of axion dark matter*, PoS COSMICWISPers (2024) 040, [[arXiv:2403.17697](#)].
- [127] L. Visinelli and P. Gondolo, *Axion cold dark matter in non-standard cosmologies*, Phys. Rev. D **81** (2010) 063508, [[arXiv:0912.0015](#)].
- [128] M. Kawasaki, K. Kohri, and N. Sugiyama, *MeV scale reheating temperature and thermalization of neutrino background*, Phys. Rev. D **62** (2000) 023506, [[astro-ph/0002127](#)].
- [129] S. Hannestad, *What is the lowest possible reheating temperature?*, Phys. Rev. D **70** (2004) 043506, [[astro-ph/0403291](#)].
- [130] F. D’Eramo, N. Fernandez, and S. Profumo, *Dark Matter Freeze-in Production in Fast-Expanding Universes*, JCAP **02** (2018) 046, [[arXiv:1712.07453](#)].
- [131] M. Badziak, K. Harigaya, M. Lukowski, and R. Ziegler, *Thermal production of astrophobic axions*, JHEP **09** (2024) 136, [[arXiv:2403.05621](#)].
- [132] D. Cadamuro, S. Hannestad, G. Raffelt, and J. Redondo, *Cosmological bounds on sub-MeV mass axions*, JCAP **02** (2011) 003, [[arXiv:1011.3694](#)].
- [133] F. Elahi, C. Kolda, and J. Unwin, *UltraViolet Freeze-in*, JHEP **03** (2015) 048, [[arXiv:1410.6157](#)].
- [134] J. Silva-Malpartida, N. Bernal, J. Jones-Pérez, and R. A. Lineros, *From WIMPs to FIMPs: Impact of Early Matter Domination*, [arXiv:2408.08950](#).
- [135] M. Viel, M. G. Haehnelt, and V. Springel, *Inferring the dark matter power spectrum from the Lyman-alpha forest in high-resolution QSO absorption spectra*, Mon. Not. Roy. Astron. Soc. **354** (2004) 684, [[astro-ph/0404600](#)].
- [136] A. Boyarsky, J. Lesgourgues, O. Ruchayskiy, and M. Viel, *Lyman-alpha constraints on warm and on warm-plus-cold dark matter models*, JCAP **05** (2009) 012, [[arXiv:0812.0010](#)].
- [137] M. Viel, G. D. Becker, J. S. Bolton, and M. G. Haehnelt, *Warm dark matter as a solution to the small scale crisis: New constraints from high redshift Lyman- α forest data*, Phys. Rev. D **88** (2013) 043502, [[arXiv:1306.2314](#)].
- [138] J. Baur, N. Palanque-Delabrouille, C. Yèche, C. Magneville, and M. Viel, *Lyman-alpha Forests cool Warm Dark Matter*, JCAP **08** (2016) 012, [[arXiv:1512.01981](#)].

- [139] V. Iršič et al., *New Constraints on the free-streaming of warm dark matter from intermediate and small scale Lyman- α forest data*, Phys. Rev. D **96** (2017), no. 2 023522, [[arXiv:1702.01764](#)].
- [140] F. D’Eramo and A. Lenoci, *Lower mass bounds on FIMP dark matter produced via freeze-in*, JCAP **10** (2021) 045, [[arXiv:2012.01446](#)].
- [141] G. Ballesteros, M. A. G. Garcia, and M. Pierre, *How warm are non-thermal relics? Lyman- α bounds on out-of-equilibrium dark matter*, JCAP **03** (2021) 101, [[arXiv:2011.13458](#)].
- [142] Q. Decant, J. Heisig, D. C. Hooper, and L. Lopez-Honorez, *Lyman- α constraints on freeze-in and superWIMPs*, JCAP **03** (2022) 041, [[arXiv:2111.09321](#)].
- [143] F. D’Eramo and A. Lenoci, *Back to the phase space: Thermal axion dark radiation via couplings to standard model fermions*, Phys. Rev. D **110** (2024), no. 11 116028, [[arXiv:2410.21253](#)].
- [144] M. Badziak and M. Laletin, *Precise predictions for the QCD axion contribution to dark radiation with full phase-space evolution*, [arXiv:2410.18186](#).
- [145] S. Antusch and V. Maurer, *Running quark and lepton parameters at various scales*, JHEP **11** (2013) 115, [[arXiv:1306.6879](#)].
- [146] G.-J. Ding and F. Feruglio, *Testing Moduli and Flavon Dynamics with Neutrino Oscillations*, JHEP **06** (2020) 134, [[arXiv:2003.13448](#)].
- [147] S. Ferrara, D. Lust, A. D. Shapere, and S. Theisen, *Modular Invariance in Supersymmetric Field Theories*, Phys. Lett. B **225** (1989) 363.
- [148] S. Ferrara, . D. Lust, and S. Theisen, *Target Space Modular Invariance and Low-Energy Couplings in Orbifold Compactifications*, Phys. Lett. B **233** (1989) 147–152.
- [149] F. Feruglio, *Are neutrino masses modular forms?*, pp. 227–266. 2019. [[arXiv:1706.08749](#)].
- [150] A. Baur, H. P. Nilles, A. Trautner, and P. K. S. Vaudrevange, *Unification of Flavor, CP, and Modular Symmetries*, Phys. Lett. B **795** (2019) 7–14, [[arXiv:1901.03251](#)].
- [151] P. P. Novichkov, J. T. Penedo, S. T. Petcov, and A. V. Titov, *Generalised CP Symmetry in Modular-Invariant Models of Flavour*, JHEP **07** (2019) 165, [[arXiv:1905.11970](#)].
- [152] A. Baur, H. P. Nilles, A. Trautner, and P. K. S. Vaudrevange, *A String Theory of Flavor and \mathcal{CP}* , Nucl. Phys. B **947** (2019) 114737, [[arXiv:1908.00805](#)].

- [153] J. Wess and J. Bagger, Supersymmetry and supergravity. Princeton University Press, Princeton, NJ, USA, 1992.
- [154] F. Feruglio, V. Gherardi, A. Romanino, and A. Titov, *Modular invariant dynamics and fermion mass hierarchies around $\tau = i$* , JHEP **05** (2021) 242, [[arXiv:2101.08718](#)].
- [155] P. P. Novichkov, J. T. Penedo, and S. T. Petcov, *Fermion mass hierarchies, large lepton mixing and residual modular symmetries*, JHEP **04** (2021) 206, [[arXiv:2102.07488](#)].
- [156] F. Feruglio, *Universal Predictions of Modular Invariant Flavor Models near the Self-Dual Point*, Phys. Rev. Lett. **130** (2023), no. 10 101801, [[arXiv:2211.00659](#)].
- [157] F. Feruglio, *Fermion masses, critical behavior and universality*, JHEP **03** (2023) 236, [[arXiv:2302.11580](#)].
- [158] G.-J. Ding, F. Feruglio, and X.-G. Liu, *Universal predictions of Siegel modular invariant theories near the fixed points*, JHEP **05** (2024) 052, [[arXiv:2402.14915](#)].